JAERI-Research
2001-016

PREMODERATOR OPTIMIZATION OF DECOUPLED HYDROGEN MODERATOR

March 2001

Masahide HARADA, Makoto TESHIGAWARA, Tetsuya KAI,
Hideaki SAKATA, Noboru WATANABE and Yujiro IKEDA

日本原子力研究所
Japan Atomic Energy Research Institute

本レポートは、日本原子力研究所が不定期に公刊している研究報告書です。
入手の問合わせは、日本原子力研究所研究情報部研究情報課（〒319-1195　茨城県那珂郡東海村）あて、お申し越し下さい。なお、このほかに財団法人原子力弘済会資料センター（〒319-1195　茨城県那珂郡東海村日本原子力研究所内）で複写による実費頒布を行っております。

This report is issued irregularly.
Inquiries about availability of the reports should be addressed to Research Information Division, Department of Intellectual Resources, Japan Atomic Energy Research Institute, Tokai-mura, Naka-gun, Ibaraki-ken 〒319-1195, Japan.

編集兼発行　日本原子力研究所

JAERI－Research 2001－016

Premoderator Optimization of Decoupled Hydrogen Moderator

Masahide HARADA※, Makoto TESHIGAWARA, Tetsuya KAI,
Hideaki SAKATA, Noboru WATANABE※※ and Yujiro IKEDA

Center for Neutron Science
Tokai Research Establishment
Japan Atomic Energy Research Institute
Tokai-mura, Naka-gun, Ibaraki-ken

(Received February 5, 2001)

An optimization study on the premoderator, the reflector material choice and a length of the liner is carried out for the design of high performance decoupled hydrogen moderator. NMTC/JAM and MCNP-4C are used for the neutronics calculation. The result indicates that, assuming premoderator dimensions and decoupling energy is controlled, the decoupled hydrogen moderator with a premoderator can provide better pulse characteristics than that without the premoderator for a Be reflector. On the selection of the reflector material, it is clearly shown that Pb and Hg reflectors give merits in using the premoderator for higher intensity and reduction of energy deposition in moderator. It is also shown that a H_2O premoderator provides a short tail while a D_2O premoderator provides the high peak intensity. Minimum liner length is evaluated to be 20 cm from the viewpoint of neutronics.

Keywords: Moderator Neutronics, Decoupled Hydrogen Moderator,
High Intensity Pulsed Spallation Neutron Source, Premoderator,
Optimization, Decoupling Energy, Reflector Material, Liner Length,
Premoderator Material

※ Post Doctoral Fellow

※※ Scientific Consultant

JAERI－Research 2001－016

非結合型水素モデレータにおけるプリモデレータの最適化

日本原子力研究所東海研究所中性子科学研究センター

原田　正英※・勅使河原　誠・甲斐　哲也

坂田　英明・渡辺　昇※※・池田　裕二郎

(2001年2月5日 受理)

高性能な非結合型水素モデレータの設計のために、プリモデレータ、反射体材質の選択、ライナー長さの最適化に関する検討を行った。中性子工学計算には、NMTC/JAM コード及びMCNP-4C コードを用いた。結果から、鉛反射体下では、デカップリングエネルギー、プレモデレータの形状及び厚さを調整することにより、ベリリウム反射体下でパルス特性を凌駕することが可能であることが示された。反射体材質の選択では、鉛反射体や水銀反射体では、プリモデレータの利用により、中性子強度が増加することやモデレータ内核発熱が軽減することが示された。また、軽水プリモデレータを使用すると、パルステールが小さくなるが、重水プリモデレータを使用するとピーク強度が大きくなることも示された。中性子工学の観点から、最小のライナー長さが得られた。

東海研究所：〒319-1195 茨城県那珂郡東海村白方白根 2-4

※　博士研究員

※※ 特別研究員

Contents

目　次

1. Introduction

The Japanese spallation neutron source (JSNS) with 1 MW power is going to be constructed as the major experimental facility under the project of JAERI (Japan Atomic Energy Research Institute) and KEK (High Energy Accelerator Research Institute). In a MW-class spallation neutron source, only hydrogen is feasible candidate for the moderator material because other candidate materials cannot be used under high radiation conditions. Three-moderators system is considered to be implemented, namely, a coupled moderator (for high intensity), an unpoisoned decoupled moderator and a poisoned decoupled moderator (for high resolution) to satisfy various neutron pulse characteristics requested by neutron scattering experiments. The decoupled moderator supplies the cold and thermal neutron pulses with a narrow peak (high peak intensity and small FWHM (Full Width of Half Maximum) with a small tail. The poisoned decoupled moderator is used to provide a narrower pulse and a smaller peak. The concept of the target moderator reflector assembly (TMRA) in JSNS is described in Ref. [1] in detail. It was suggested in the coupled moderator study that a premoderator provided the high intensity and reduced the heat deposition of the moderator in a Pb (lead) reflector without sacrificing pulse shape characteristics, and that a premoderator extension was very effective [2]. In the decoupled moderator, it is well known that the Pb reflector gives longer neutron pulse tails (longer decay times) in the slowing-down region than the Be (beryllium) reflector. This is because Pb reflector has a longer slowing-down time than Be one. It has already been thought that a premoderator for a decoupled H_2 moderator gave no merit (or attenuation) in the neutron time-integrated and pulse peak intensities with the Be reflector. On the other hand, the study indicated that a premoderator provided the high intensity without sacrificing pulse shape in the Pb reflector [3,4]. To realize a better neutronic performance, an optimization of premoderator geometry and thickness is necessary and a choice of the premoderator material is important. Further, as the premoderator effect is closely related to decoupling energies which are sensitive to a tail of pulse, it should be taken into account. Length of a liner, which is important on viewpoint of both neutronics and engineering, is dependent on premoderator extension.

In viewing above, we have studied the premoderator optimization for the decoupled hydrogen moderator for following items:

(1) Optimization of premoderator geometry and thickness,

(2) Decoupling energy dependence of premoderator effect,

(3) Reflector material dependence of premoderator effect,

(4) Premoderator material dependence,

(5) Influence of premoderator on moderator induced neutron flux,

(6) Optimization of liner length,

(7) Comparison of simple model with detailed model.

2. Calculation Model and Method

2.1. Basic Model of Calculation

For the neutronic calculation, a high-energy nucleon-meson transport code "NMTC/JAM" (neutron energy range above 20 MeV) [5-9] and a neutron transport Monte Carlo code "MCNP-4C" (below 20 MeV) [10] were used. Cross section data used in the MCNP-4C code is based on the JENDL-3 evaluated library [11,12]. The calculation model is schematically shown in **Figs. 1** (3-dimensional view) and **2** (2-dimensional view). For an unpoisoned decoupled liquid H_2 moderator, the dimension is W 12 cm x H 12 cm x L 5 cm, we assumed that the H_2 is the normal hydrogen at 20 K and the ortho/para ratio is 3:1. The moderator was placed under the mercury target which had a dimension of W 40 cm x H 8 cm x L 60 cm. As shown in **Fig. 3**, the size of the viewed surface of moderator is 10 x 10 cm^2 and the vertical position of near side is same as that of near side of moderator. Instead of vessels of the target and the moderator, gaps are taken into account. Proton beams of 3 GeV, 25 Hz and 333 μA (13 μA/pulse) were injected into the target, as shown in **Fig. 3**. The proton incident beam profile of 13 x 5 cm^2 rectangle shape with a uniform distribution was assumed. The moderator was decoupled with the reflector by 3 mm thick B_4C (boron carbide) decoupler. The same material and thickness as decoupler were used for liner. By controlling the B_4C density, the decoupling energy was adjusted down to 1 eV. The premoderator of H_2O (light water) surrounding the moderator and extending to the neutron beam hole was placed at the outside of decoupler shown in **Fig. 2**. The reflector material studied in this report was mainly Pb. The size of it is 120 cm in diameter and 120 cm in height, as shown in **Fig. 4**. A neutron detector is located at the 2 m distance from the moderator surface. In this study, one decoupled moderator is modeled in the calculation, and other moderators were neglected.

2.2. Model of Each Study

2.2.1. Optimization of Premoderator Geometrical Shape and Thickness

Geometrical shapes and thickness of premoderator are optimized in terms of the neutron intensity gain. In the calculation model, the premoderator is divided into 2 parts, *i.e.*, the main premoderator and the extended premoderator. Eight values of thickness or length, which define geometry of these premoderators are used as parameters. The values are shown in **Fig. 5**. In the analysis, firstly, parameter ① is searched and fixed to get the highest neutron intensity. Next, parameter ② is searched to get the highest neutron intensity with the fixed parameter ①. Other parameter is searched in the same way and 8 parameters are determined to obtain the highest neutron intensity.

2.2.2. Decoupling Energy Dependence

Increase of the decoupling energy in the Pb reflector improves pulse tail to be small strongly though the neutron intensity decreases. This effect is smaller than that in the Be reflector. Neutron intensity and FWHM are calculated with different decoupling energies. Decoupling energies are changed by using B_4C or Cd (cadmium) decouplers with the fixed thickness and by adjusting their density.

2.2.3. Reflector Material Dependence

Candidates of the reflector material are Pb and Be at present moment. Teshigawara et al. indicated that Hg (mercury) could be one of a good reflector material that provided a sharp pulse tail because Hg has a function as a weak decoupler and is available to use itself as coolant [13]. For the Be and the Hg reflectors, geometry and thickness of premoderator are optimized with change of decoupling energies by the same way in the case of Pb reflector (see Sec.2.2.2).

2.2.4. Premoderator Material Dependence

Along with H_2O, D_2O (heavy water) is a candidate for the premoderator. Ooi et al. indicated that D_2O was effective on neutronic performance for a decoupled moderator [14]. In this study, the pulse shape with the H_2O premoderator is compared with that with the D_2O premoderator. Thickness of the D_2O premoderator optimized in the Ref. [14] is used as 2.0 cm for ①, 5.0 cm for ② and ④, and 0 cm for others.

2.2.5. Influence of Premoderator on Moderator Induced Neutron Flux

We consider the softening effect which leads to a neutron intensity gain. Energy and time spectra of neutrons coming to the moderator through each moderator surface are calculated for the Pb reflector in case without premoderator, with the H_2O premoderator and the D_2O premoderator. Geometrical shape and thickness of these premoderators used are optimized in each case.

2.2.6. Optimization of Liner Length

We suppose that the length of liner is related to the premoderator extension. Though a long liner makes the pulse tail small, a short liner is preferred on the view point of engineering because cooling of liner becomes critical. Thus, the pulse shape is calculated by changing the length of liner. As shown in **Fig. 6**, assumed liner lengths are 0 cm (no liner case), 20 cm (liner case of 20 cm in length) and 50 cm (all liner case). In this calculation, geometrical shape and thickness of the premoderator are optimized at decoupling energy of

1eV.

2.2.7 Comparison of Simple Model with Detailed Model

As mentioned in the calculation, we have adopted simple models. However, as the practical system is so complicated, we have to examine a possible difference between the simple model and a more realistic detailed model, for example, for reflector missing due to other moderator beam holes. Sakata et al. indicated that the reflector missing caused a possible intensity loss of about 10 % for the coupled moderator [15]. The calculated result in the simple model is compared with these in the detailed model [16].

3. Results and Discussions

3.1 Optimization of Premoderator Geometrical Shape and Thickness

Figure 7 shows a gain of neutron intensity with increase of the premoderator extension and thickness. The intensity is normalized to that with no premoderator. **Figure 7** shows that the premoderator at near side to the target gives more gain of intensity than that at far side with respect to the target, and the main premoderator is more effective on the intensity gain than the extended premoderator. The optimized premoderator gave an increase up to 40 %. Parameter set of the optimized premoderator is shown in **Table 1**. **Figure 8** shows the pulse shape for the optimized premoderator, comparing to that of no premoderator. It is clear that the premoderator increases the peak intensity without sacrificing any pulse tail. As shown in **Table 2**, the heat deposition in the moderator is reduced by 37% from that of no premoderator. Other merits by using the premoderator are found in the separation between the moderator and the target. Larger separation between the moderator and the target, in general, provides a better S/N ratio for the neutron scattering experiment. In this case, the neutron intensity becomes smaller generally. However, the premoderator can automatically provide the larger separation without loss of the neutron intensity. Maekawa et al. indicated that the background caused by a fast neutron flux for the experiments was reduced with increasing the separation [17].

3.2 Decoupling Energy Dependence

Figure 9 shows the neutron intensity with increase of the decoupling energy for no premoderator, the optimized premoderators at decoupling energy 1eV, and the optimized premoderators at different decoupling energies. The optimization results in addition to no decoupler case, which is equivalent to the coupled moderator case [2], are summarized in **Table 1**. Optimized premoderators provide the highest intensity at each decoupling energy, and the intensity decreases with increase of the decoupling energy. As the decoupling energy

increases, the neutron intensity in both the case with the premoderator and the one without the premoderator similarly decreases. Especially, for the optimized premoderator at the decoupling energy of 1eV, the premoderator causes a loss of neutron intensity at decoupling energy 100 eV. This is because the softening effect for the neutron flux is too much. Though by using the optimized premoderator at a corresponding decoupling energy gives a gain of neutron intensity, the gain is decreased with increasing decoupling energy. **Figure 10** shows the peak intensity at different decoupling energies in both no premoderator and optimized premoderators with corresponding decoupling energies. Though FWHM is not changed much with increase of the decoupling energy, the peak intensity shows the same tendency of the neutron intensities as shown in **Fig. 10**. **Figure 11** indicates that the pulse tail component decreases with increase of the decoupling energy in no premoderator and the optimized premoderator. There is no significant difference in the pulse tail in each case.

Figure 12 shows the pulse shape with the Pb reflector using the optimized premoderator and with the Be reflector using no premoderator as a function of the decoupling energy. At the same decoupling energy, the pulse tail with the Pb reflector is longer than that with the Be reflector. However, when decoupling energy is adjusted for the Pb reflector to be the same tail shape for the Be reflector, the peak intensity with the Pb reflector is higher than that with the Be reflector.

3.3 Reflector Material Dependence

In the same way for the Pb reflector case, premoderators were optimized for the Be and Hg reflector at each decoupling energy. The parameters are summarized in **Tables 3** and **4**. As shown in **Table 2**, heat deposition can be also reduced by using premoderator in these reflectors. The J values, which are defined as the neutron intensity integrated in the time and the Maxwellian energy region, increase by using the premoderator shown in **Fig. 13**. For the Be reflector, it is clear that the premoderator gives little merit in increase of the intensity. On the other hand, for both the Hg and the Pb reflectors, intensity gains by using the premoderator, and the decoupling energy dependency show the almost same tendency and the premoderators give large merit in increasing intensity.

3.4 Premoderator Material Dependence

The time-integrated neutron intensity for the H_2O premoderator is 10 % lower than that for the D_2O premoderator. As shown in **Fig. 14**, the peak intensity for H_2O is also 5 % lower than that for D_2O. On the other hand, FWHM and pulse tail for H_2O are better than those for D_2O. Incidentally, separation between the target and the moderator with the D_2O premoderator (parameter ① is 2.5cm) is larger than that with the H_2O premoderator (parameter ① is 1,5cm).

However, studies on other factors, such as a reflector coolant effect, location balance to other moderators, and engineering problems (for example, increase of D_2O transfer line by using D_2O) and so on, the choice of H_2O or D_2O should be further investigated.

3.5 Influence of Premoderator on Moderator Induced Neutron Flux

Figure 15 shows the time-integrated neutron spectral intensity of neutron current to the moderator at the moderator surface with no premoderator for the Pb reflector. It is clear that the neutron current to the moderator through the near side surface is about 10 times higher than those through other surfaces and the energy spectrum is very hard. **Figure 16** shows the time-integrated neutron current at surfaces to the moderator without and with H_2O and D_2O premoderators. It is obvious that premoderator makes energy spectra of moderator-induced neutron soft and neutron intensity around 1eV increases with thickness of H_2O and D_2O premoderators increases. It is shown that the D_2O premoderator provides weaker softening than the H_2O premoderator. We guess that the reason for the smaller intensity gain of the H_2O premoderator than that of the D_2O premoderator lies in a neutron absorption of hydrogen and the strong softening effect of H_2O.

3.6 Optimization of Liner Length

Figure 17 shows the pulse shape at 50 meV with change in the length of the liner. Pulse in the no liner case has much worse tail than that in the all-liner case. It is concluded that no liner system shouldn't be taken into account. However, pulse tail with the liner of 20 cm length and the all-liner is the same amplitude and the same decay time. Therefore, we consider that the liner of 20 cm in length is adequate.

3.7 Comparison of Simple Model with Detailed Model

Figures. 18 and **19** show energy spectrum and time structure of the neutron pulse for the simple model and the detailed model, respectively. Both the neutron intensity and peak intensity for the detailed model are 30 % lower than those for the simple model in the whole energy region. On the other hand, FWHM in the detailed model is same as that of the simple model. The pulse shapes in the both cases are shown in **Fig. 20.** There is almost no difference in the pulse tail. These results suggest that pulse characteristic is adequately estimated by the simple model and the detailed model.

4. Conclusions

The result for optimization of premoderator indicates that assuming that premoderator and decoupling energy is controlled to obtain best performance in the case of the Pb reflector, the decoupled hydrogen moderator with the premoderator can provide better

pulse characteristics than that without premoderator for the Be reflector.

For the reflector material, it is obvious that, though the premoderator in the Be reflector gives little merit for intensity gain, the premoderators in Pb and Hg reflector cases give large effectiveness. With respect to the energy deposition in the moderator and the separation between the target and the moderator, there are large merits by using the premoderator.

The H_2O premoderator provides short tails while the D_2O premoderator provides high peak intensity. However it is not yet the time to determine the premoderator material. Calculated neutron current to the moderator through the near target side is the highest intensity.

In addition, length of liner of 20 cm from the tip of extended premoderator is almost adequate.

Moreover, neutron intensity in the case of the detailed model is 30 % lower than that of the simple model and there is no difference in the pulse shapes between the simple model and the detailed model.

Acknowledgements

The authors would like to thank staffs of Center for Promotion of Computational Science and Engineering in JAERI for providing a parallel computer system, called PC Cluster for exclusive use of the present calculation. And the authors would like to thank Prof. Kiyanagi and Mr. Ooi in Hokkaido University for helpful discussions and advises. The authors would like to thank Prof. Furusaka, Prof. Kawai and Prof. Arai of KEK for helpful discussions and advises.

References

[1] The joint project team of JAERI and KEK: JAERI-Tech 99-056 (1999); KEK Report 99-4 (1999); JHF-99-3 (1999).

[2] Kai, T., et al.: to be published in Proc. International Collaboration of Advanced Neutron Source XV, (2001).

[3] Harada, M., et al.: "Premoderator extension effect for a decoupled hydrogen moderator", JAERI-Research 2000-01 (2000) [in Japanese].

[4] Harada, M, et al.: "Optimization of decoupled hydrogen moderator", to be published in Proc. International Collaboration of Advanced Neutron Source XV, (2001).

[5] Nakahara, Y., and Tsutsui, T.: JAERI-M 82-198 (1982) (in Japanese).

[6] Takada, H., et al.: JAERI-Data/Code 98-005 (1998).

[7] Nara, Y., et al.: Phys. Rev. **C61**, 024901 (1999).

[8] Niita, K.: Proc. 1999 Symp. Nucl. Data, JAERI-Conf 2000-05, 98 (2000).

[9] Niita, K., et al.: to be published in Proc. International Collaboration of Advanced Neutron Source XV, (2001).

[10] Briesmeister, J. F., (Ed.): LA12625 (1993).

[11] Nakagawa, T.: J. Nucl. Sci. Technol., **32**, 1259 (1995).

[12] Shibata, K., et al.: J. Nucl. Sci. Technol. **34**, 503 (1997).

[13] Teshigawara, M., et al.: to be published in Proc. International Collaboration of Advanced Neutron Source XV, (2001).

[14] Ooi, M., et al.: to be published in Proc. International Collaboration of Advanced Neutron Source XV, (2001).

[15] Sakata, H., et al.: to be published in Proc. International Collaboration of Advanced Neutron Source XV, (2001).

[16] Teshigawara, M., et al.: private communication.

[17] Maekawa, F., et al.: to be published in Proc. International Collaboration of Advanced Neutron Source XV, (2001).

Table 1 Optimized premoderator thickness at each decoupling energy with the Pb reflector

Decoupling Energy (eV)	Decoupler	Premoderator parameter							
		1 (cm)	2 (cm)	3 (cm)	4 (cm)	5 (cm)	6 (cm)	7 (cm)	8 (cm)
*(0.0)		2.5	2.5	2.5	2.5	2.5	15.0	2.5	2.5
0.3	Cd	2.0	2.0	0.5	2.0	1.5	7.5		
1.0	B4C	1.5	1.5	1.0	1.5	1.0	5.0	0.5	0.5
10.0	B4C	1.0	1.0	0.5	1.0	1.0	5.0	0.5	0.5
100.0	B4C	0.5	0.5	0.5	0.5	1.0	2.5		

*: Ref. [2]

Table 2 Heat deposition in the moderator for each case

Reflector	Premoderator	Heat deposition (kWt/MW)		
		NMTC*1	MCNP*2	Total
Pb		0.14	1.13	1.28
	H2O	0.09	0.70	0.78
Be		0.11	0.72	0.83
	H2O	0.12	0.56	0.68
Hg		0.14	0.96	1.09
	H2O	0.10	0.67	0.76

*1: NMTC: Other high-energy component

*2: MCNP: Neutron component of energy range below 20 MeV

Table 3 Optimized premoderator thickness at each decoupling energy with the Be reflector

Decoupling Energy (eV)	Decoupler	Premoderator parameter							
		1 (cm)	2 (cm)	3 (cm)	4 (cm)	5 (cm)	6 (cm)	7 (cm)	8 (cm)
*(0.0)		2.5	1.0	1.0	1.0	2.5	3.0	1.0	1.0
0.3	Cd	1.5				0.5	5.0		
1.0	B4C	1.0	0.5		0.5	0.5	5.0		
10.0	B4C				(No intensity gain)				
100.0	B4C				(No intensity gain)				

*: Ref. [15]

Table 4 Optimized premoderator thickness at each decoupling energy with the Hg reflector

Decoupling Energy (eV)	Decoupler	Premoderator parameter							
		1 (cm)	2 (cm)	3 (cm)	4 (cm)	5 (cm)	6 (cm)	7 (cm)	8 (cm)
0.3	Cd	1.5	2.0	0.5	2.0	1.5	10.0		
1.0	B4C	1.0	1.0	1.0	1.0	0.5	10.0	0.5	

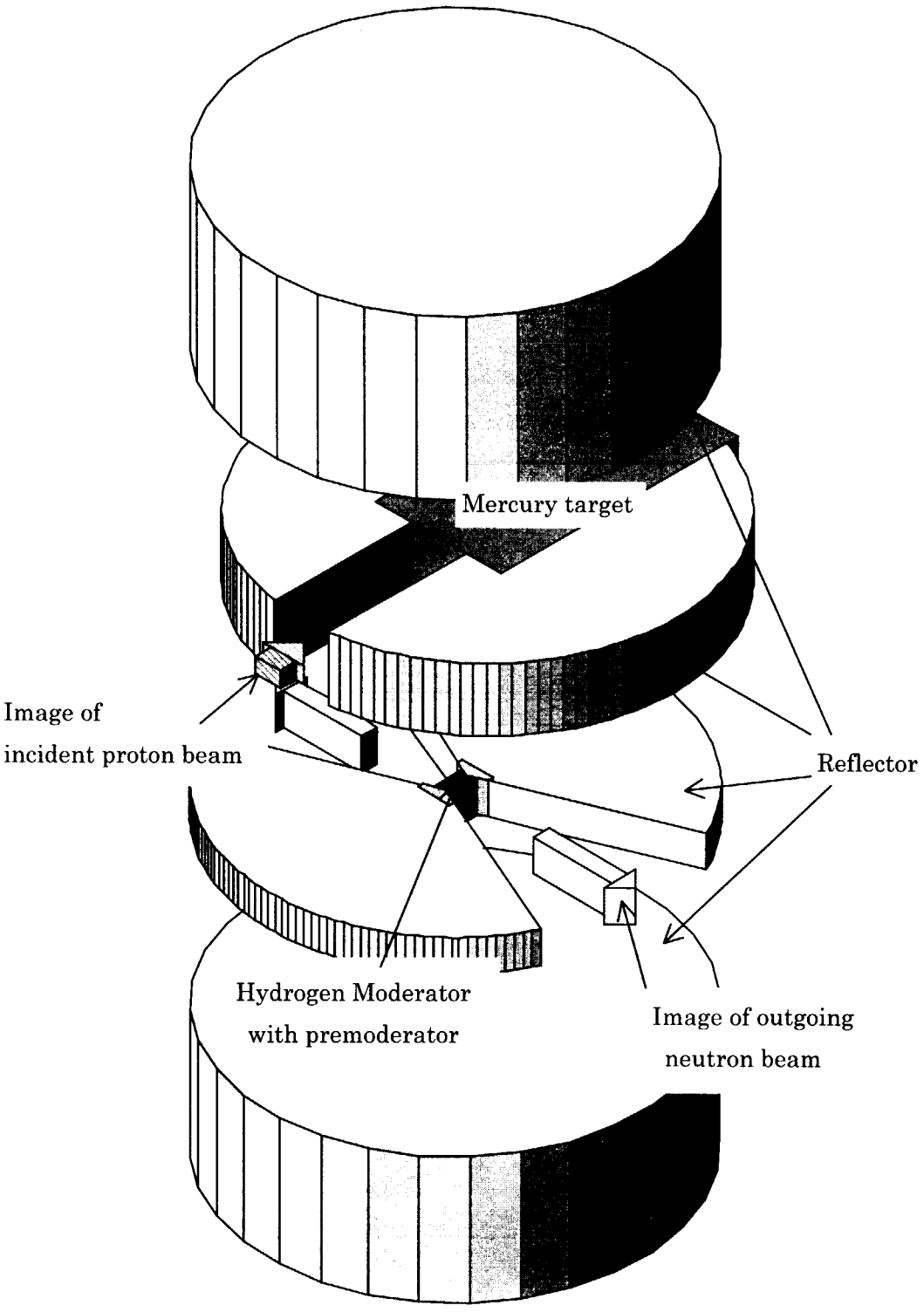

Fig. 1 Illustration of the simple model of the target moderator reflector assembly
Each component is stacked into one system.

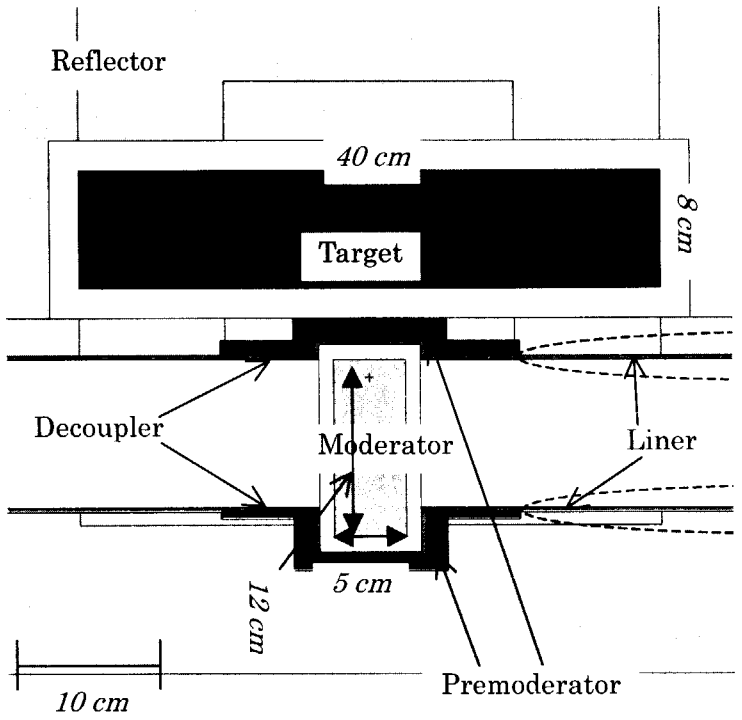

(a): Vertical cross sectional view (perpendicular to proton beam direction)

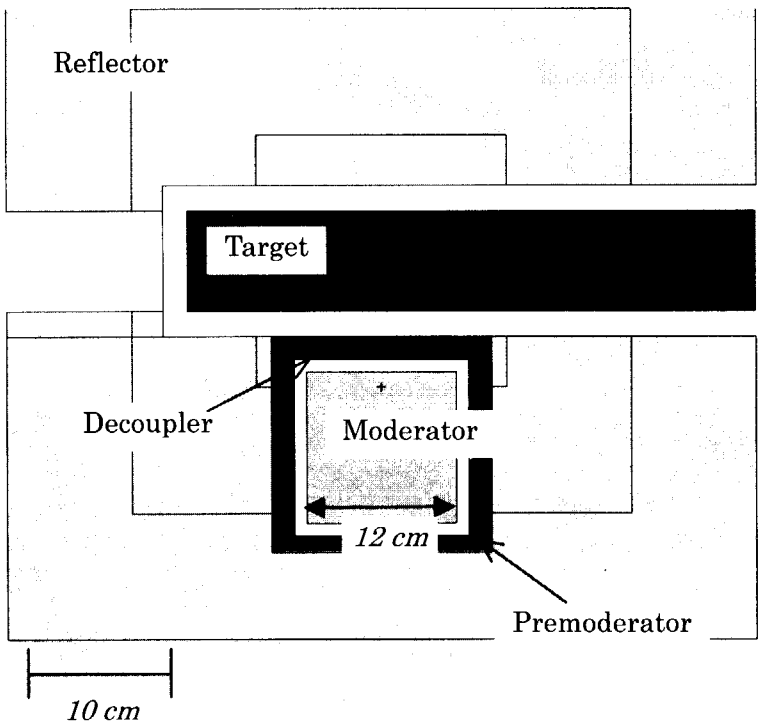

(b): Vertical cross sectional view (perpendicular to neutron beam direction)

Fig. 2 Schematic calculation model (target, moderator and premoderator) (1/2).

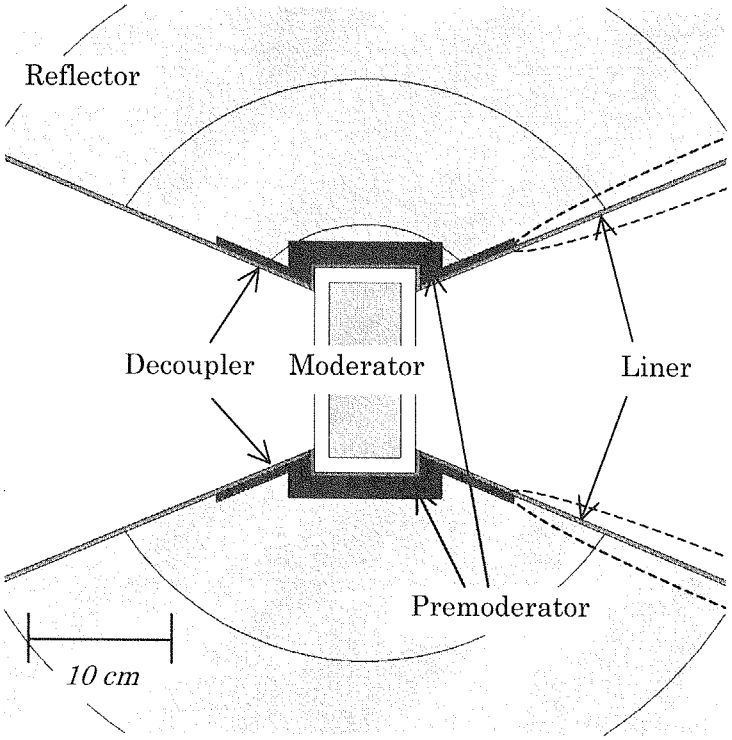

(c): Horizontal cross sectional view

Fig. 2 Schematic calculation model (target, moderator and premoderator) (2/2).

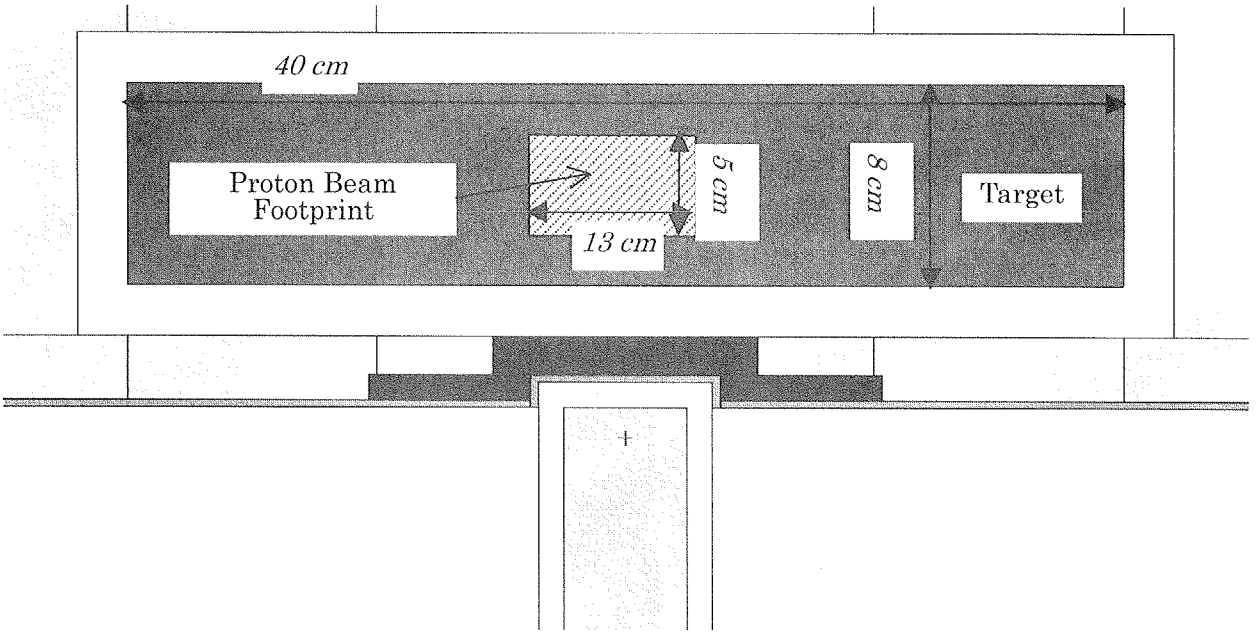

(a): Vertical cross sectional view of target and proton beam footprint
(perpendicular to proton beam direction)
These positions are centered.

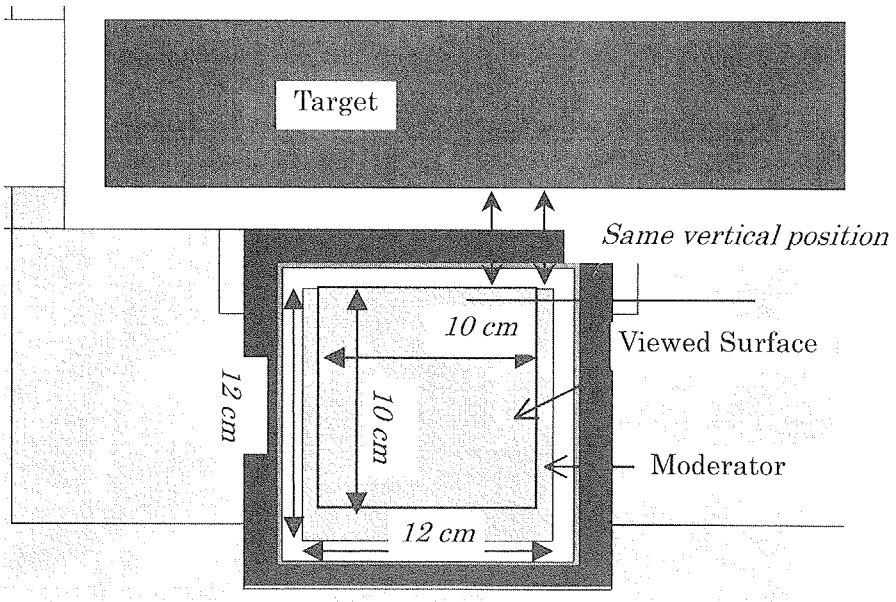

(b): Vertical cross sectional view of moderator and viewed surface
(perpendicular to neutron beam direction)
Vertical positions of top of these are same.

Fig. 3 Sizes and positions of proton beam footprint and viewed surface.

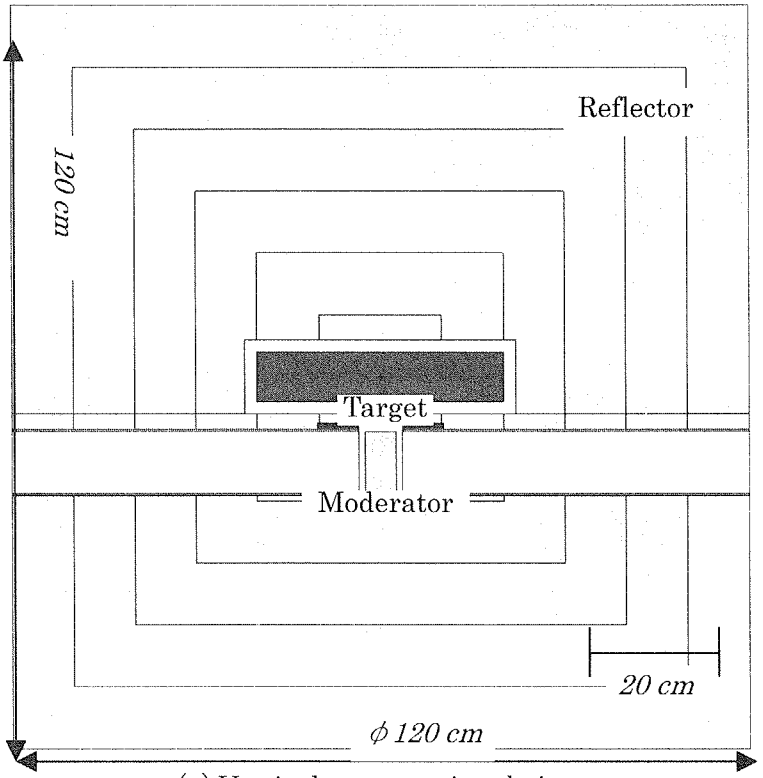

(a) Vertical cross sectional view

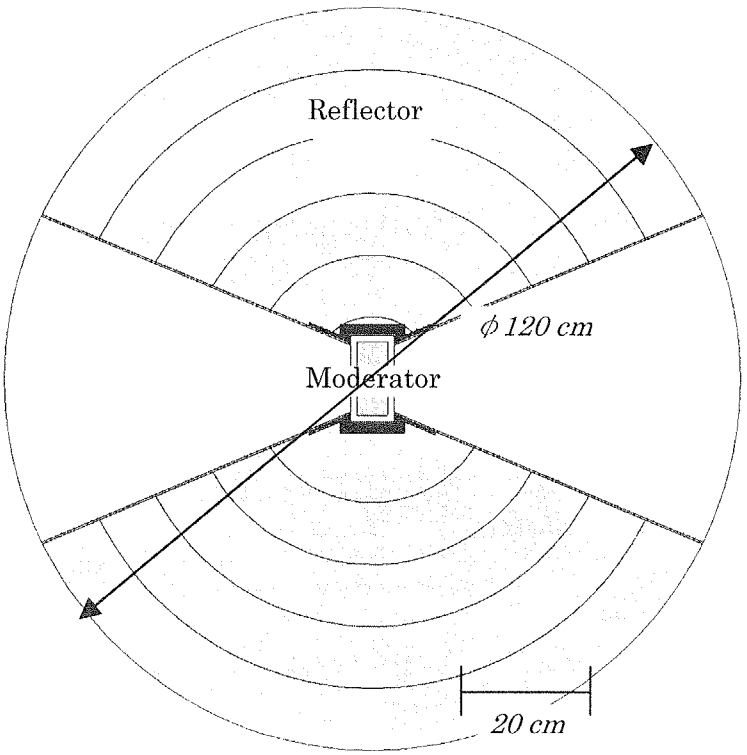

(b) Horizontal cross sectional view

Fig. 4 Schematic calculation model (reflector).
Reflector is cylinder shape.

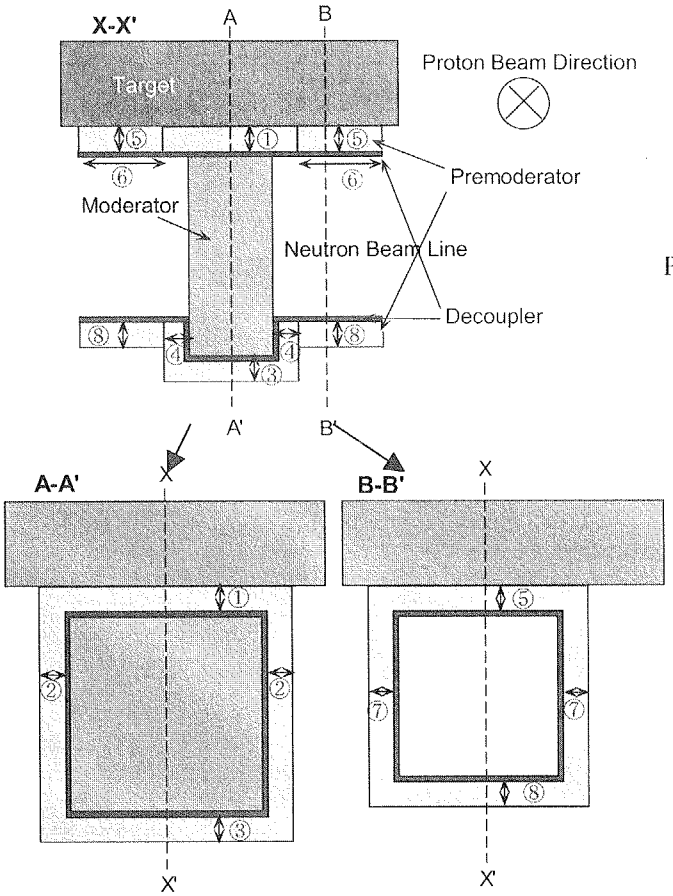

Parameterized geometrical shape and thickness

(Main premoderator)

① Near side premoderator thickness

② Side premoderator thickness

③ Far side premoderator thickness

④ Beam extracted side premoderator thickness

(Extended premoderator)

⑤ Near side extended premoderator thickness

⑥ Extension length

⑦ Side extended premoderator thickness

⑧ Far side extended premoderator thickness

Fig. 5 Eight parameters to define premoderator geometrical shape and thickness.

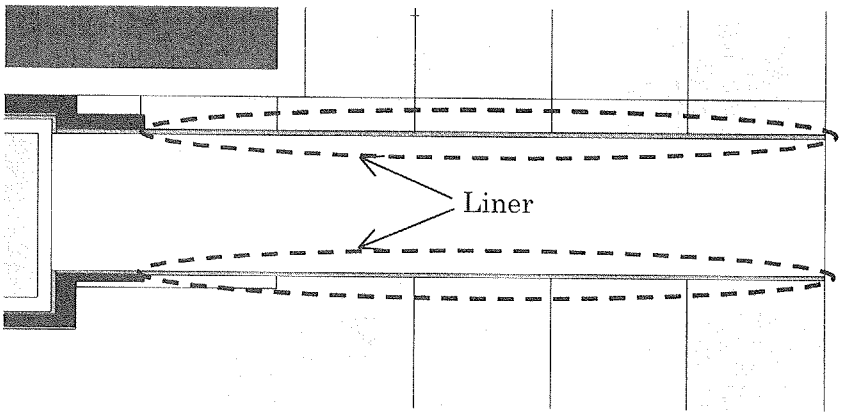

(a) All liner Case
Length of the liner is 50 cm.

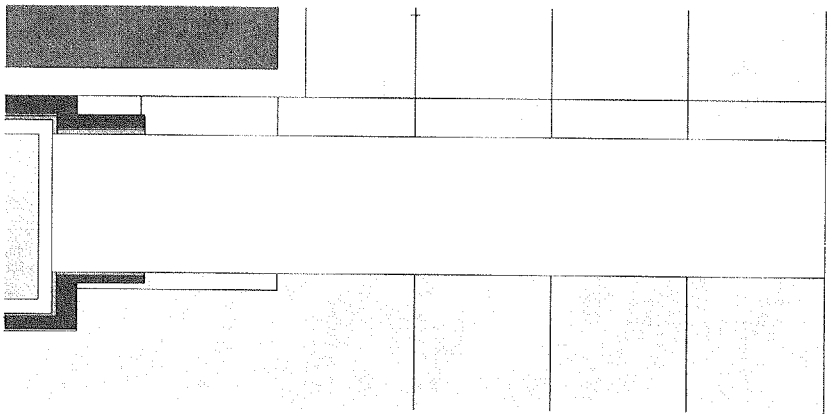

(b) No liner case
Length of the liner is 0 cm.

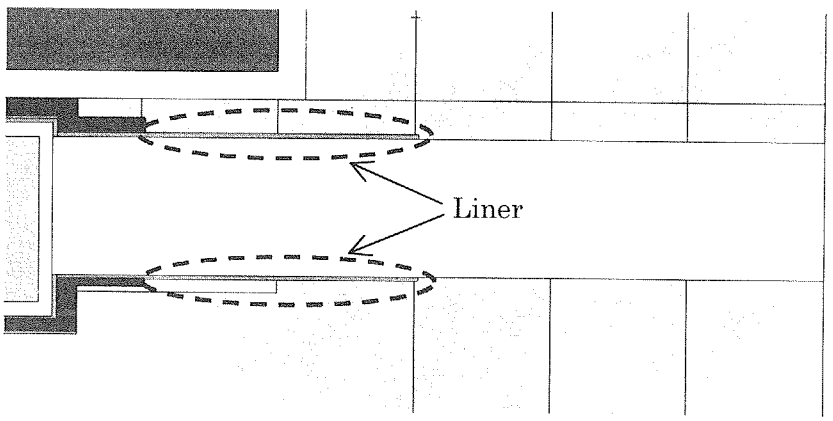

(c) Liner case of 20 cm in length
Length of the liner is 20 cm.

Fig. 6 Schematic view of Liner in each calculation.

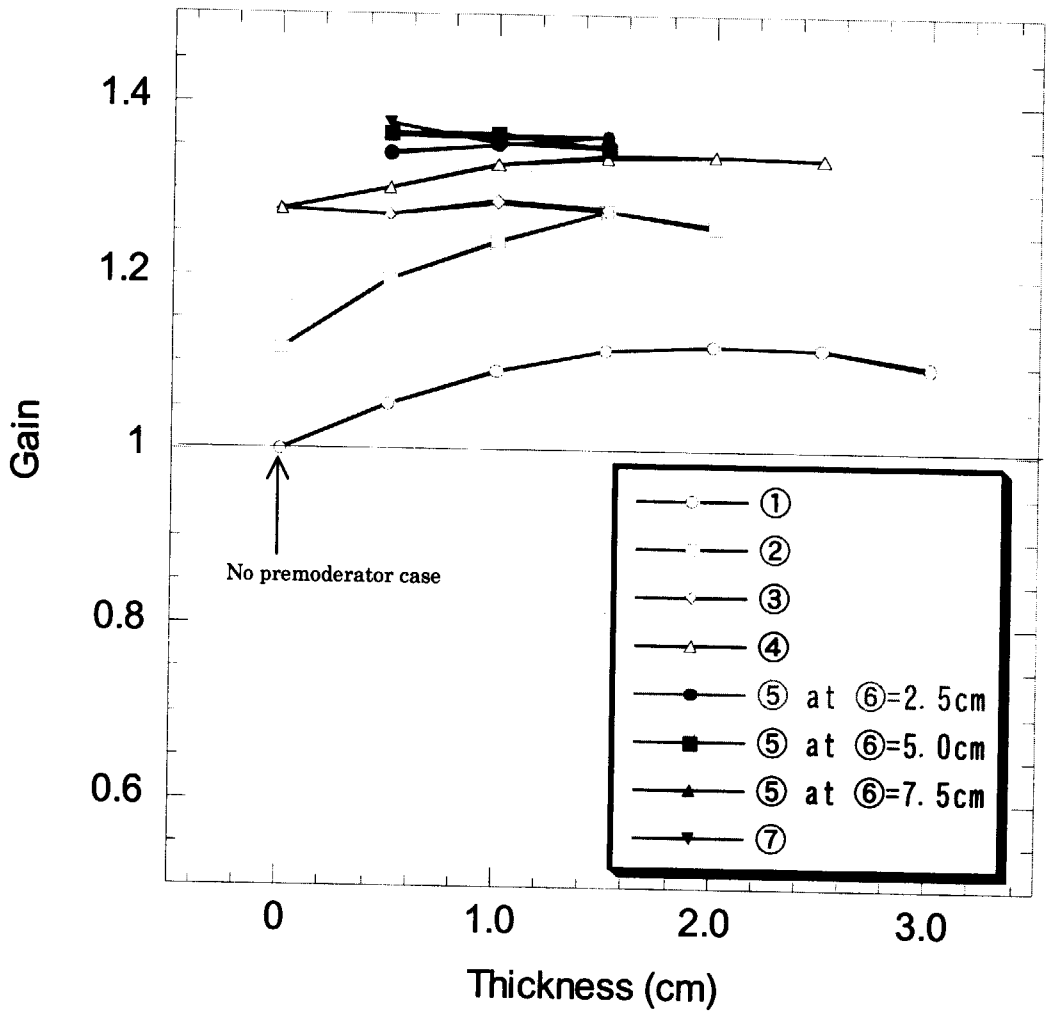

Fig. 7 Premoderator geometrical shape and thickness dependence of time-integrated neutron intensity in the energy region from 50 meV to 200 meV in the Pb reflected case at decoupling energy of 1eV.

These values are normalized to neutron intensity in the case with no premoderator. Each number in legend in the figure corresponds with the premoderator parameter shown in the Fig. 5.

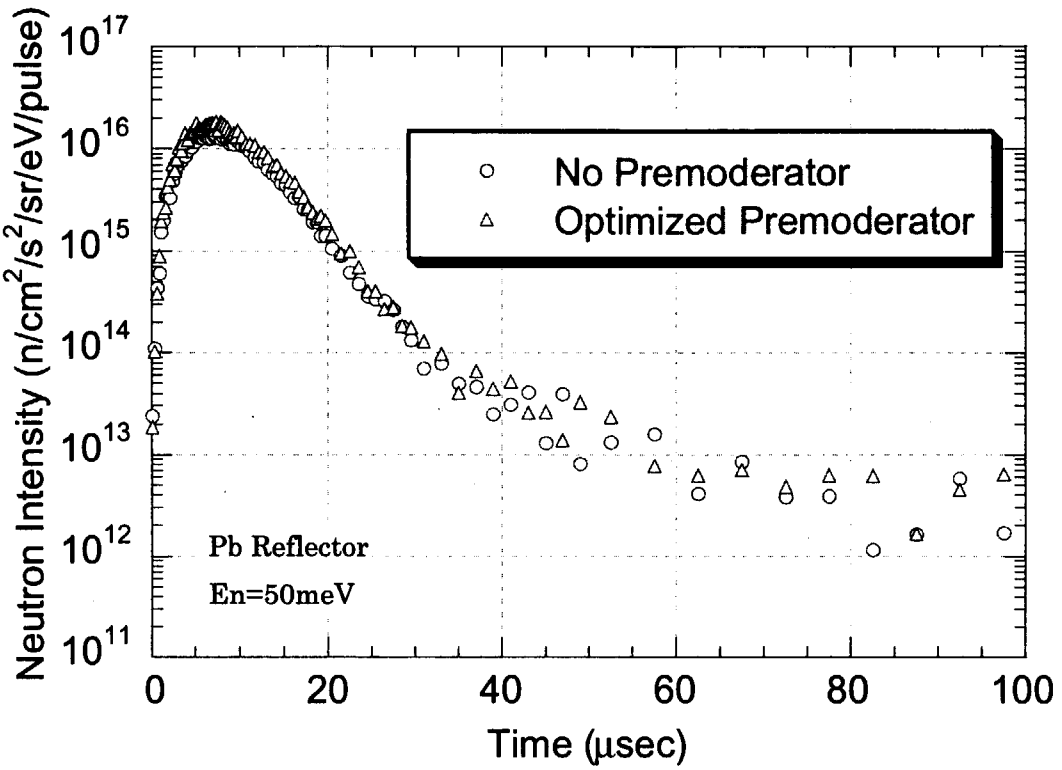

Fig. 8 Comparison of pulse shape in optimized premoderator case with that in no premoderator case at En=50 meV in the Pb reflector. Decoupling energy is 1eV.

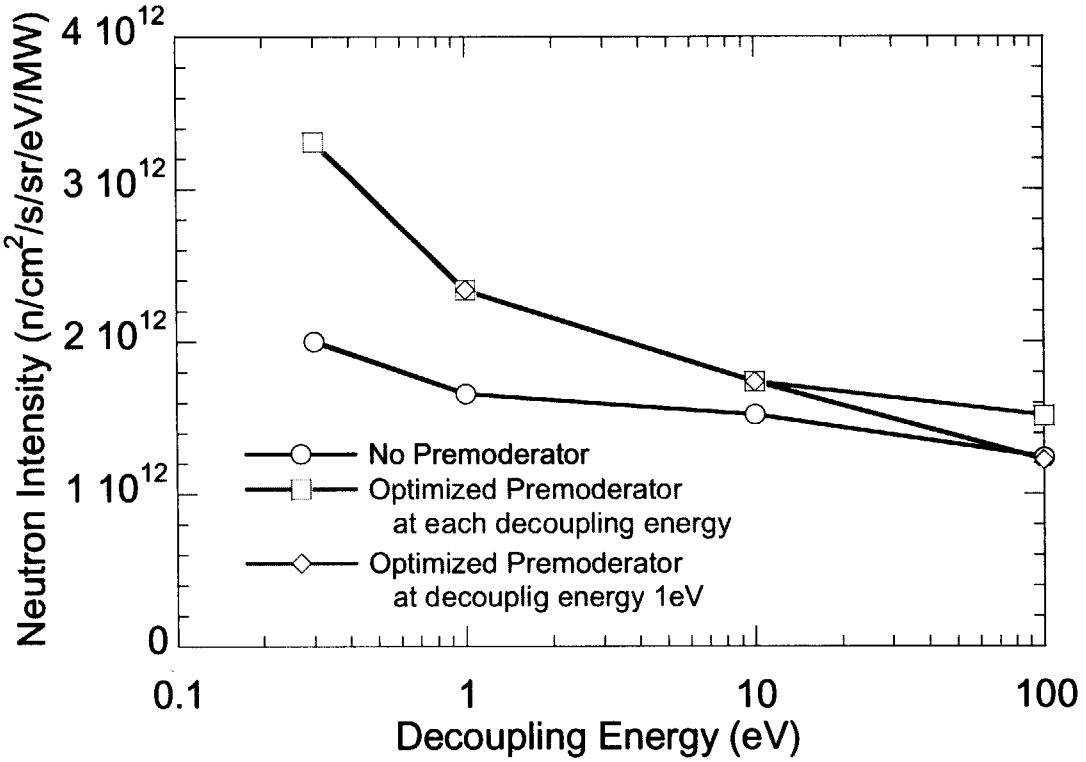

Fig. 9 Decoupling energy dependence of time-integrated neutron intensity at En=100 meV in the case of Pb reflector with no premoderator, optimized premoderator at each decoupling energy and optimized premoderator at decoupling energy 1eV.

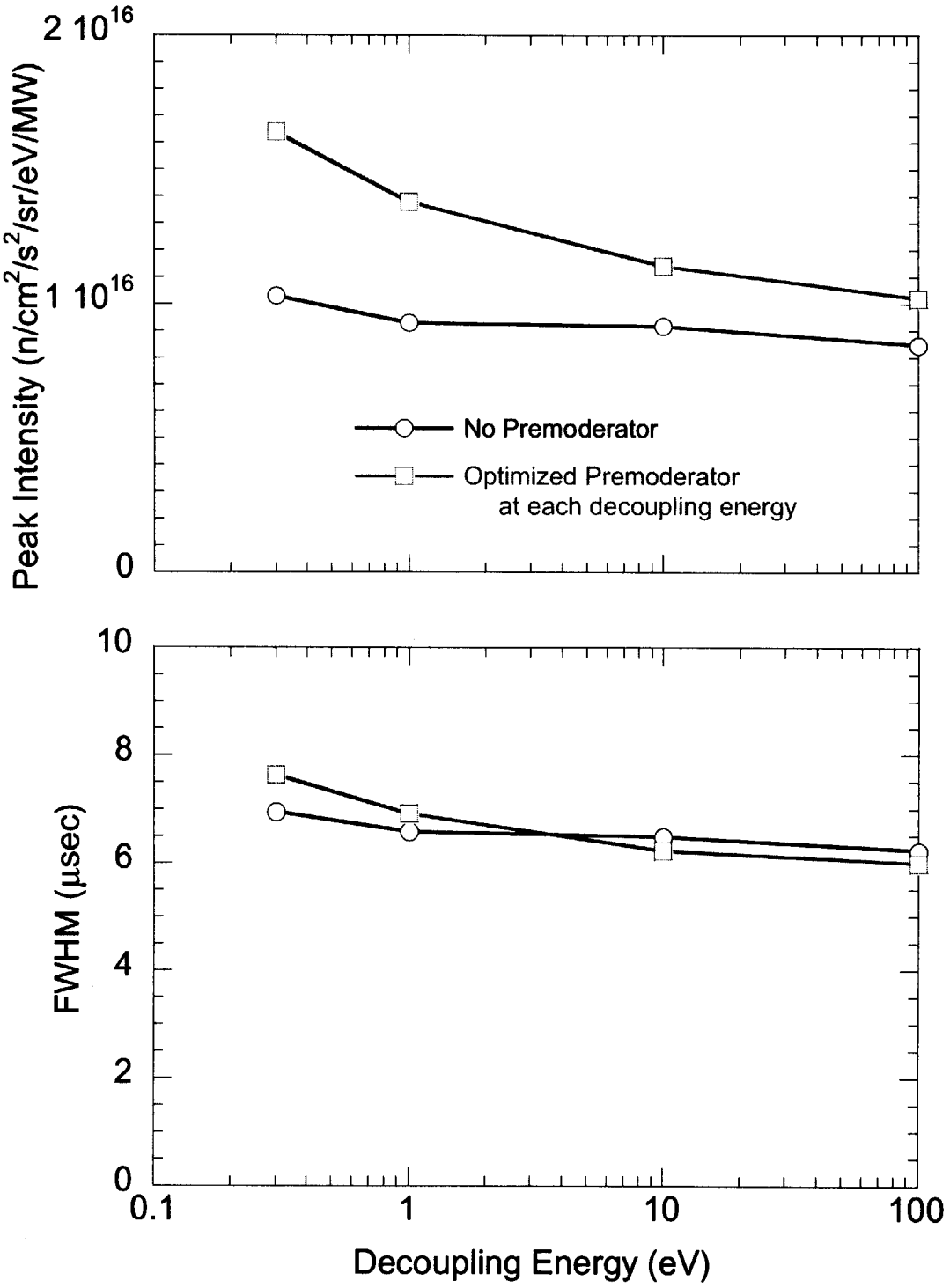

Fig. 10 Decoupling energy dependence of peak intensity and FWHM at En=100 meV in the case of Pb reflector with no premoderator and optimized premoderator at each decoupling energy.

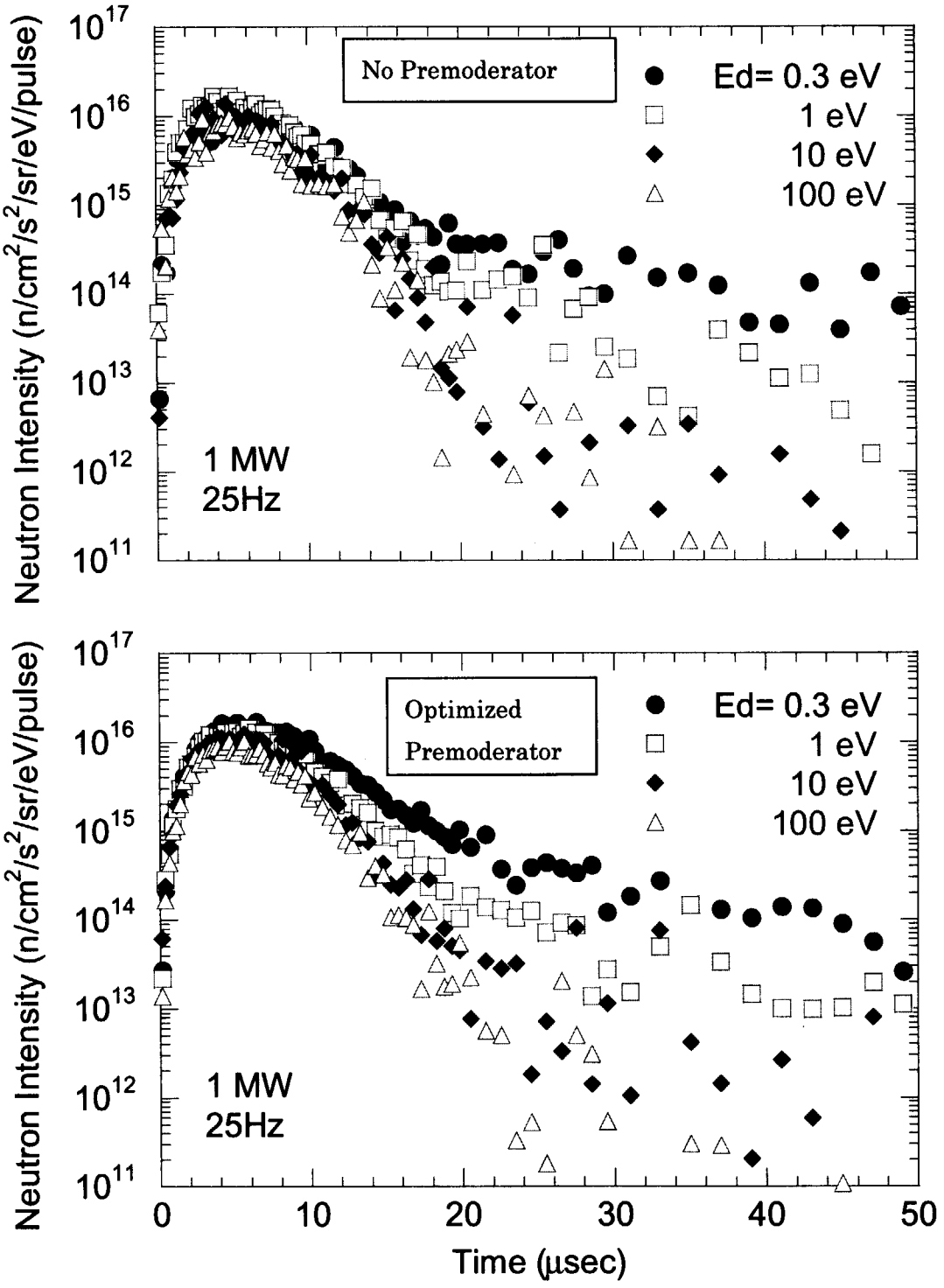

Fig. 11 Decoupling energy dependence of pulse shape at En=100 meV in the case of Pb reflector with no premoderator and optimized premoderator at each decoupling energy.
(Upper: No premoderator, Lower: Optimized premoderator)

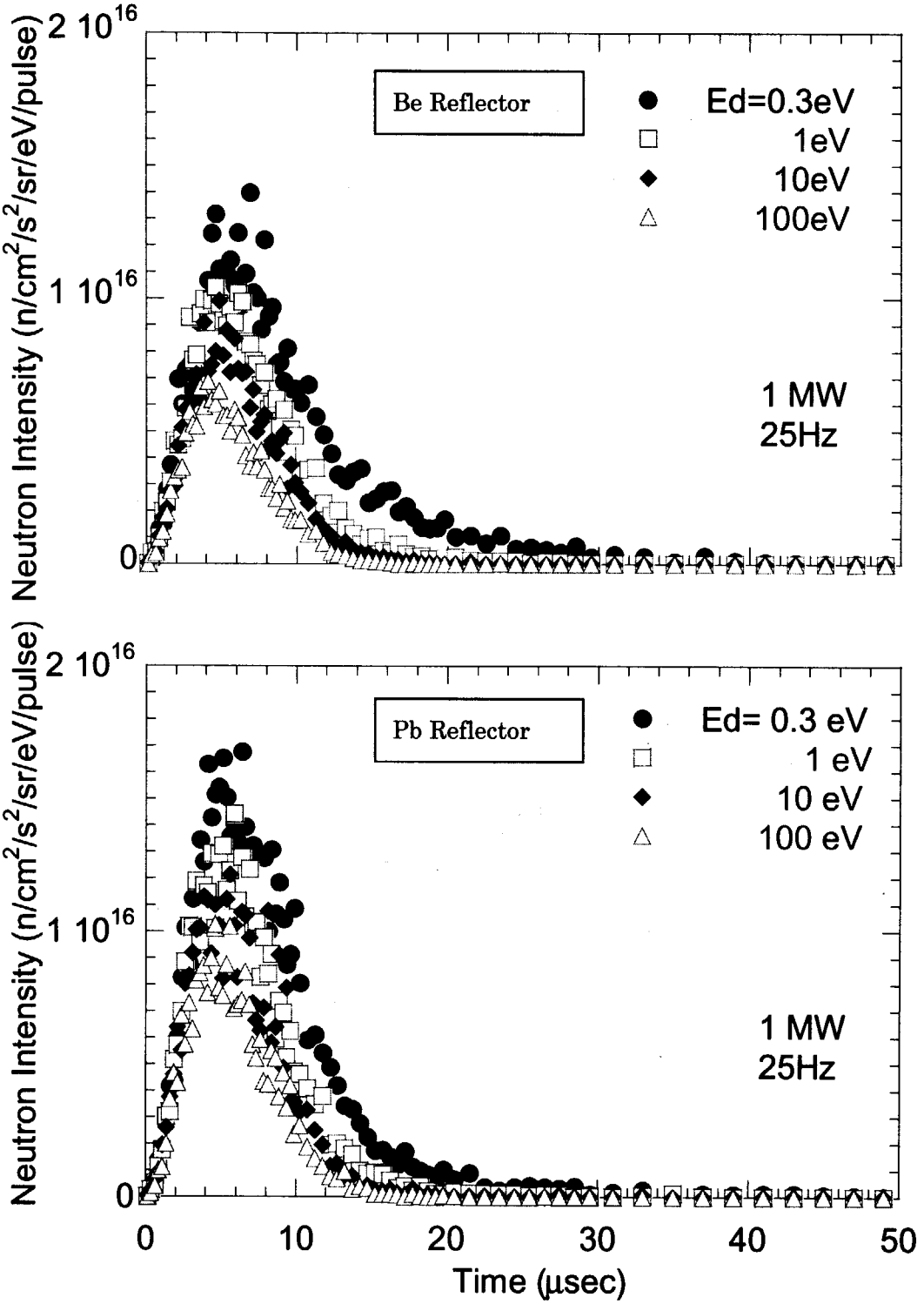

(a) Linear scale

Fig. 12 Decoupling energy dependence of neutron intensity at En=100 meV in the case of Pb reflector with premoderator and Be reflector with no premoderator. (1/2)

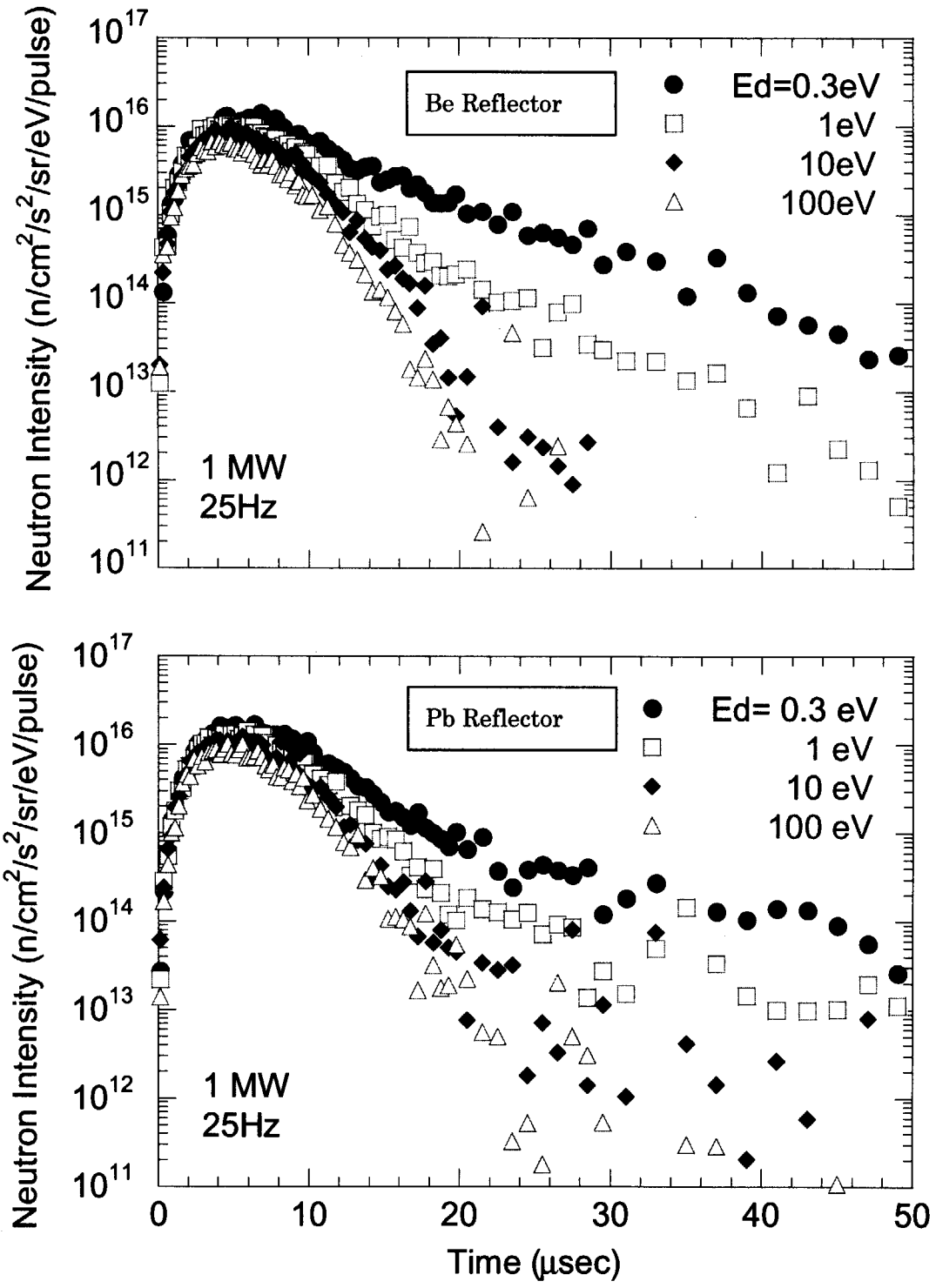

(b) Logarithm scale

Fig. 12 Decoupling energy dependence of neutron intensity at En=100 meV in the case of Pb reflector with premoderator and Be reflector with no premoderator. (2/2)

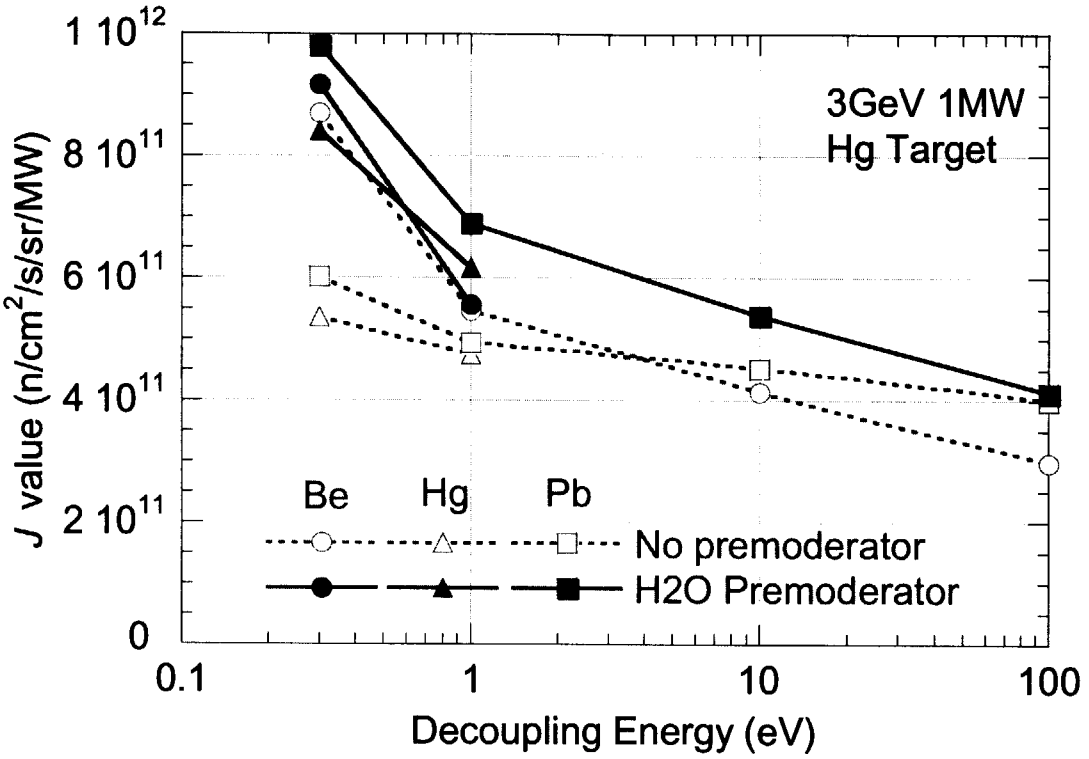

Fig. 13 Decoupling energy dependence of neutron intensity integrated in the time and the Maxwellian energy region (J value) in the case of the Pb, Be and Hg reflector with no and H_2O premoderator.

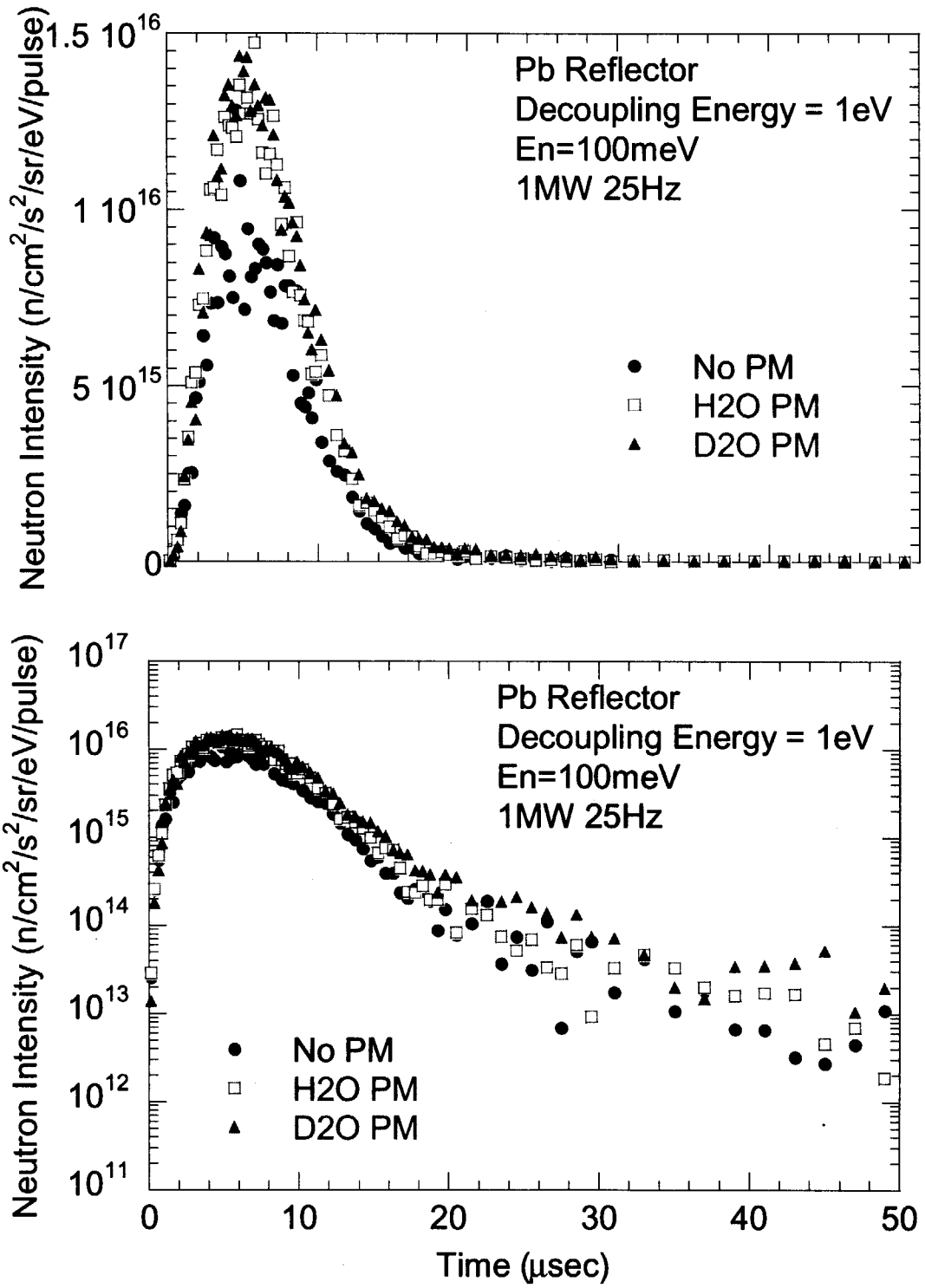

Fig. 14 Comparison of time structure in the case without, with H_2O premoderator and with D_2O premoderator at En=100 meV.
(Upper: Linear scale, Lower: Logarithm scale)

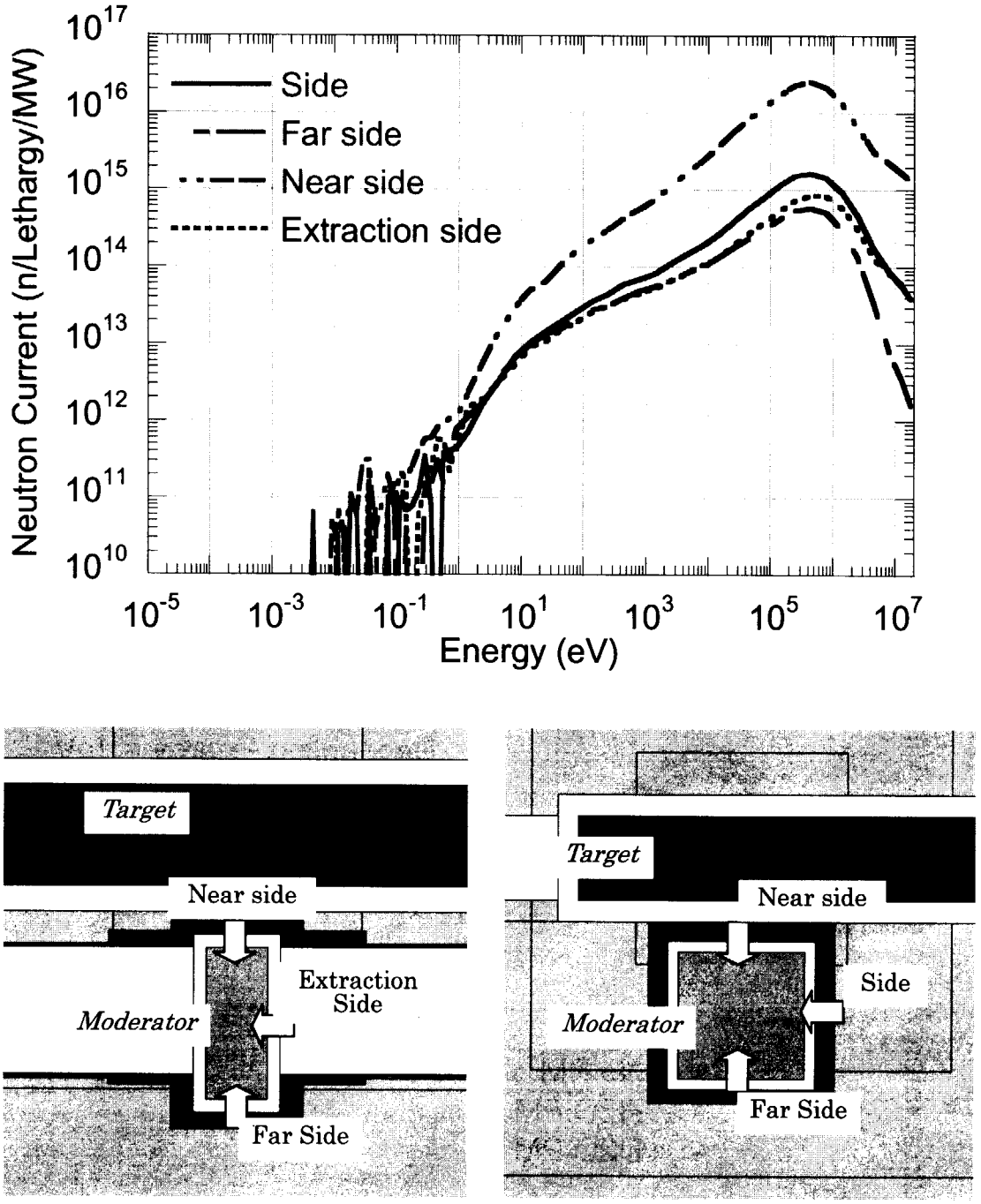

Fig.15 Neutron current to the moderator at each moderator surface with no premoderator
Position of each surface is shown in lower figure.

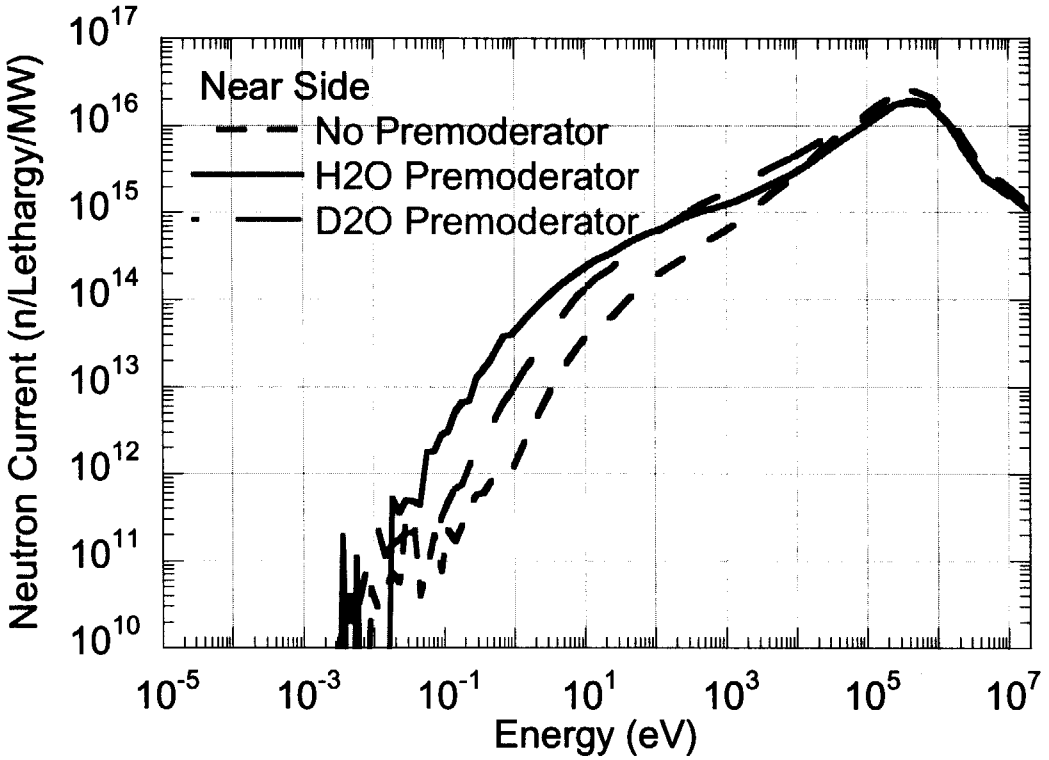

(a) Near side surface

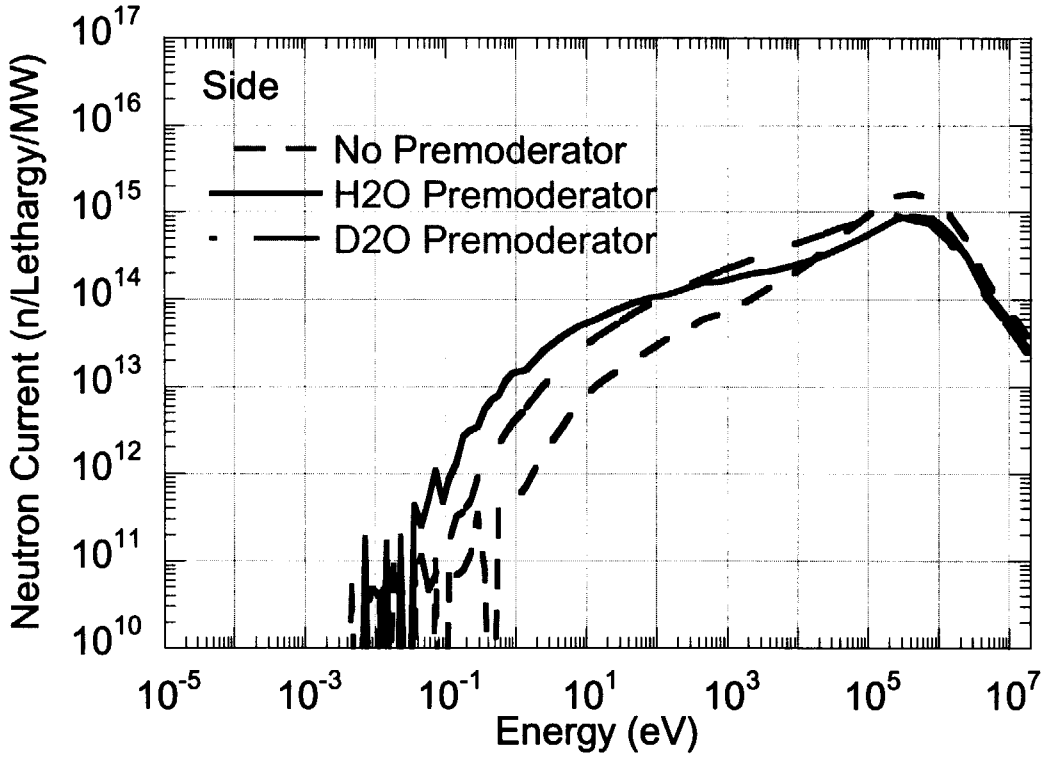

(b) Side surface

Fig.16 Neutron current to moderator at each moderator surface without premoderator, with H_2O premoderator and with D_2O premoderator. (1/2)

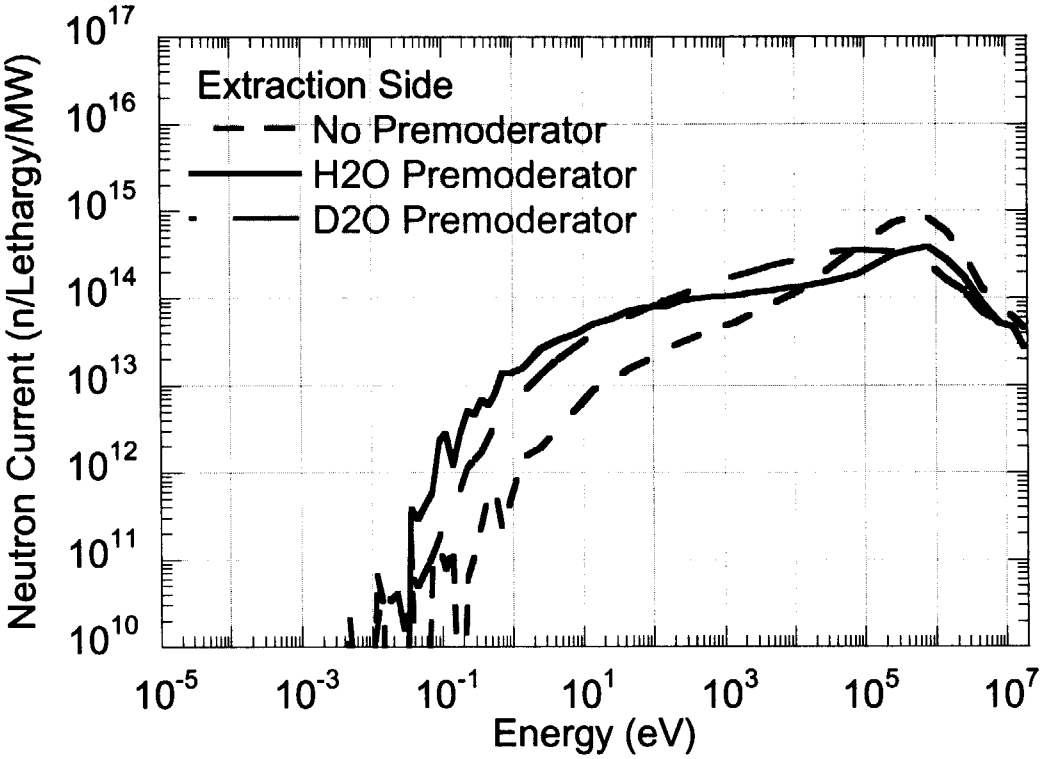

(c) Extraction side surface

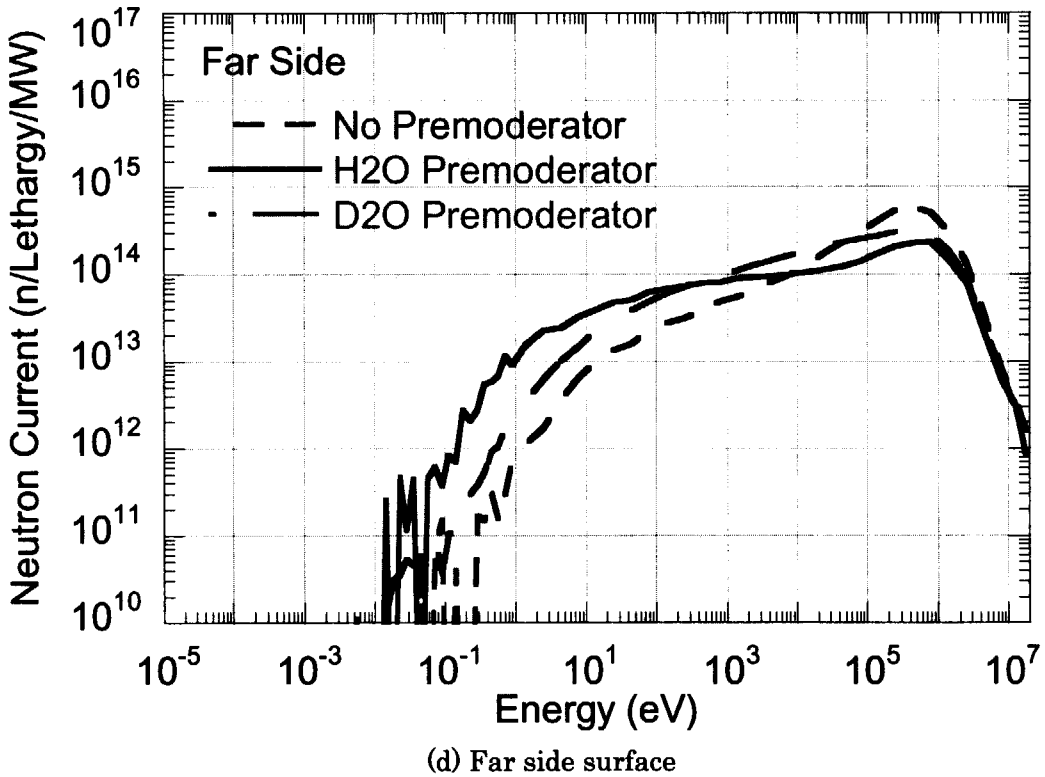

(d) Far side surface

Fig.16 Neutron current to moderator at each moderator surface without premoderator, with H_2O premoderator and with D_2O premoderator. (2/2)

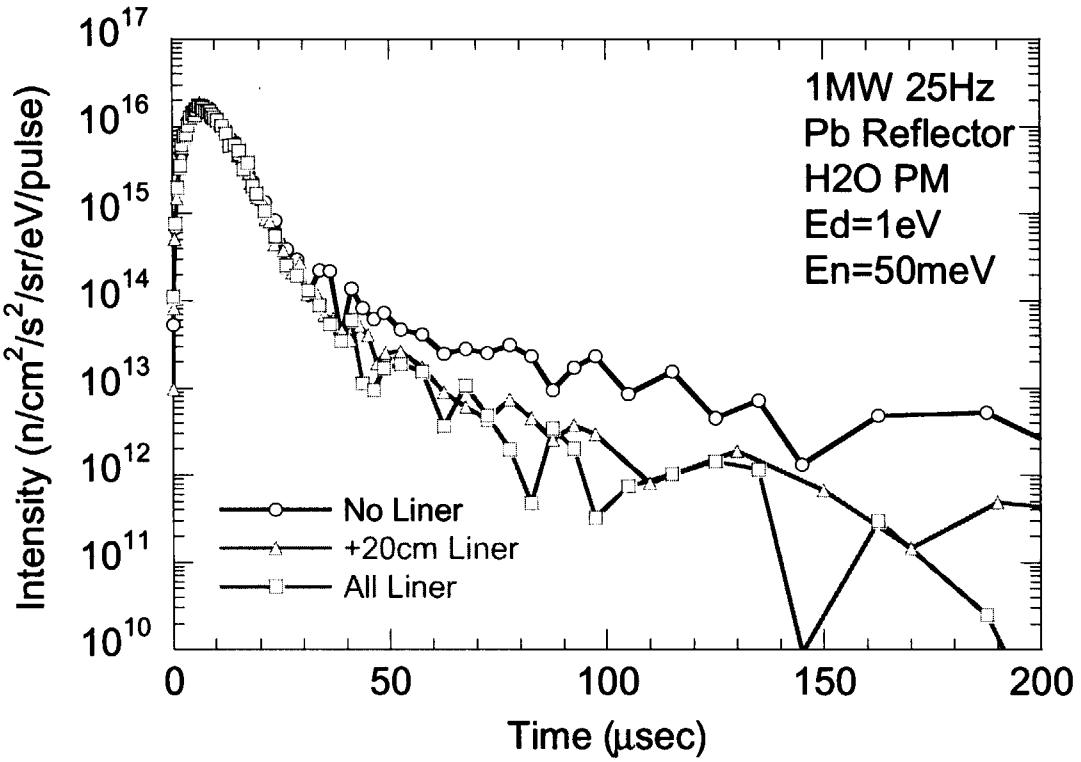

Fig. 17 Pulse shape with no liner, all liner and 20 cm length liner at En=50 meV.

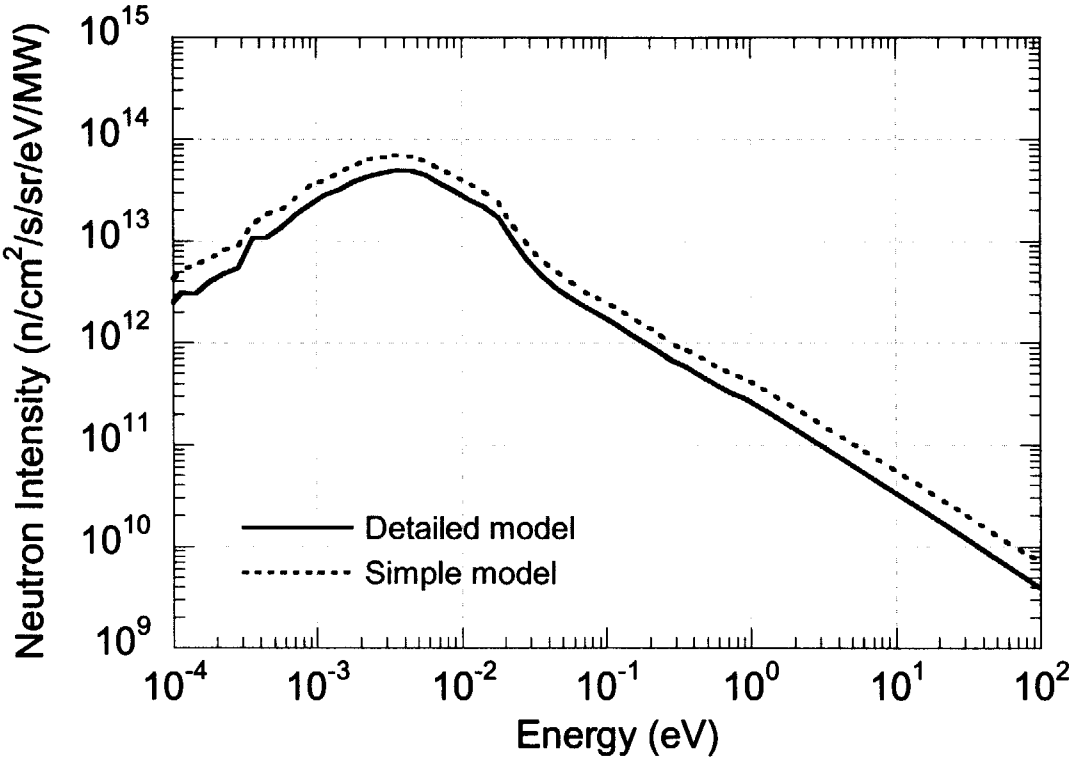

Fig. 18 Comparison of energy spectrum calculated in the simple model with that in the detailed model in decoupled hydrogen moderator.

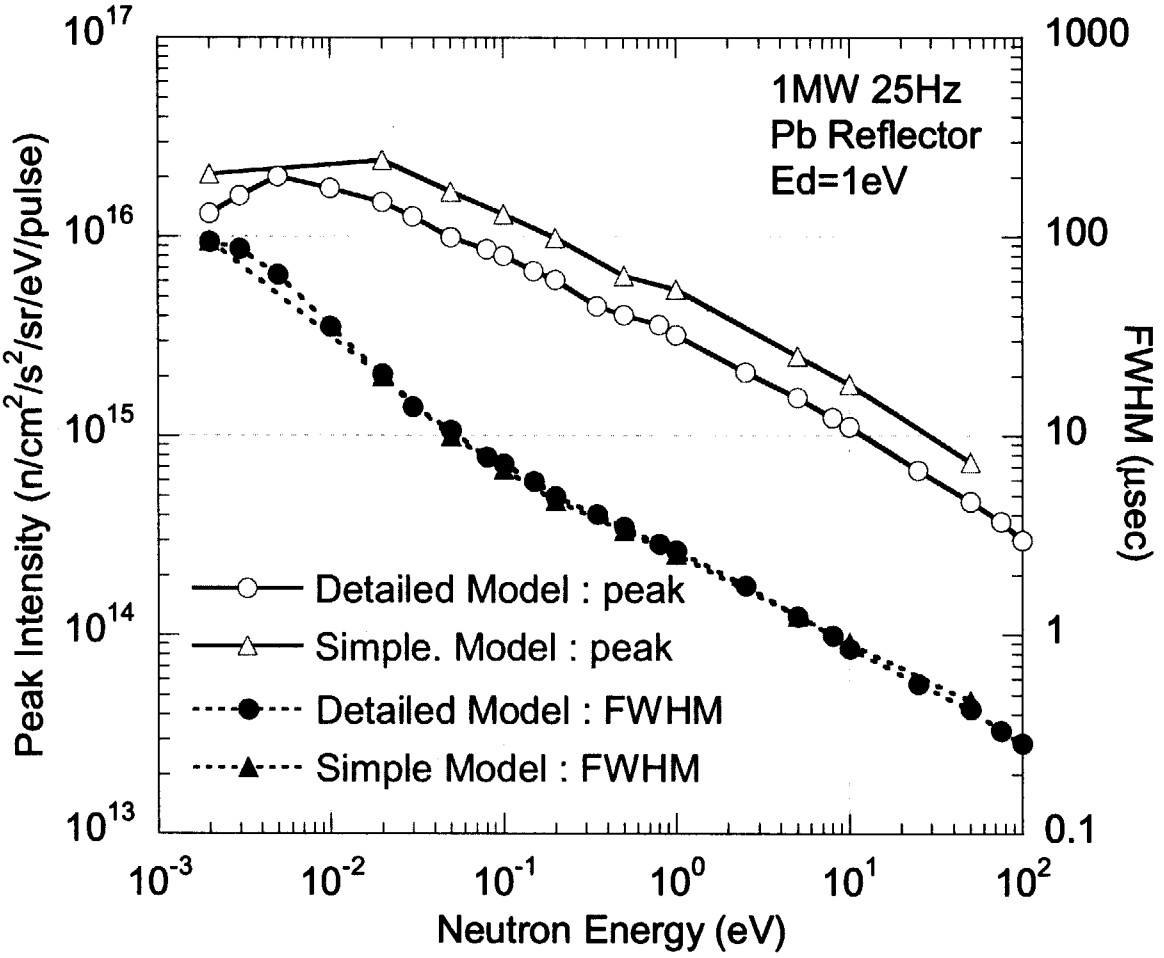

Fig. 19 Comparison of peak intensity and FWHM calculated in the simple model with that in the detailed model.

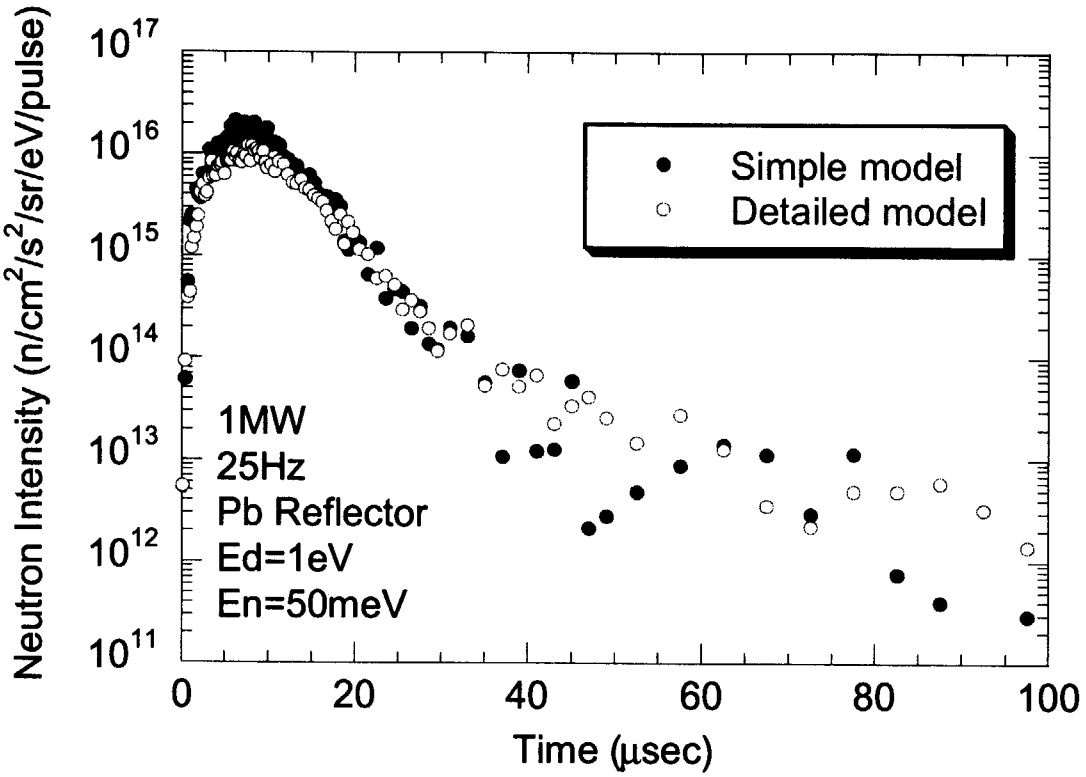

Fig. 20 Comparison of pulse shape calculated in the simple model with that in the detailed model.
Neutron energy is 50 meV.

国際単位系 (SI) と換算表

表 1　SI 基本単位および補助単位

量	名称	記号
長さ	メートル	m
質量	キログラム	kg
時間	秒	s
電流	アンペア	A
熱力学温度	ケルビン	K
物質量	モル	mol
光度	カンデラ	cd
平面角	ラジアン	rad
立体角	ステラジアン	sr

表 2　SI と併用される単位

名称	記号
分，時，日	min，h，d
度，分，秒	°，′，″
リットル	l，L
トン	t
電子ボルト	eV
原子質量単位	u

1 eV = 1.60218 × 10^{-19} J

1 u = 1.66054 × 10^{-27} kg

表 3　固有の名称をもつ SI 組立単位

量	名称	記号	他の SI 単位による表現
周波数	ヘルツ	Hz	s^{-1}
力	ニュートン	N	$m \cdot kg/s^2$
圧力，応力	パスカル	Pa	N/m^2
エネルギー，仕事，熱量	ジュール	J	N·m
工率，放射束	ワット	W	J/s
電気量，電荷	クーロン	C	A·s
電位，電圧，起電力	ボルト	V	W/A
静電容量	ファラド	F	C/V
電気抵抗	オーム	Ω	V/A
コンダクタンス	ジーメンス	S	A/V
磁束	ウェーバ	Wb	V·s
磁束密度	テスラ	T	Wb/m^2
インダクタンス	ヘンリー	H	Wb/A
セルシウス温度	セルシウス度	℃	
光束	ルーメン	lm	cd·sr
照度	ルクス	lx	lm/m^2
放射能	ベクレル	Bq	s^{-1}
吸収線量	グレイ	Gy	J/kg
線量当量	シーベルト	Sv	J/kg

表 4　SI と共に暫定的に維持される単位

名称	記号
オングストローム	Å
バーン	b
バール	bar
ガル	Gal
キュリー	Ci
レントゲン	R
ラド	rad
レム	rem

1 Å = 0.1 nm = 10^{-10} m

1 b = 100 fm^2 = 10^{-28} m^2

1 bar = 0.1 MPa = 10^5 Pa

1 Gal = 1 cm/s^2 = 10^{-2} m/s^2

1 Ci = 3.7 × 10^{10} Bq

1 R = 2.58 × 10^{-4} C/kg

1 rad = 1 cGy = 10^{-2} Gy

1 rem = 1 cSv = 10^{-2} Sv

表 5　SI 接頭語

倍数	接頭語	記号
10^{18}	エクサ	E
10^{15}	ペタ	P
10^{12}	テラ	T
10^{9}	ギガ	G
10^{6}	メガ	M
10^{3}	キロ	k
10^{2}	ヘクト	h
10^{1}	デカ	da
10^{-1}	デシ	d
10^{-2}	センチ	c
10^{-3}	ミリ	m
10^{-6}	マイクロ	μ
10^{-9}	ナノ	n
10^{-12}	ピコ	p
10^{-15}	フェムト	f
10^{-18}	アト	a

（注）

1. 表 1 — 5 は「国際単位系」第 5 版，国際度量衡局 1985 年刊行による。ただし，1 eV および 1 u の値は CODATA の 1986 年推奨値によった。
2. 表 4 には海里，ノット，アール，ヘクタールも含まれているが日常の単位なのでここでは省略した。
3. bar は，JIS では流体の圧力を表わす場合に限り表 2 のカテゴリーに分類されている。
4. EC 閣僚理事会指令では bar，barn および「血圧の単位」mmHg を表 2 のカテゴリーに入れている。

換算表

力	N(=10^5 dyn)	kgf	lbf
	1	0.101972	0.224809
	9.80665	1	2.20462
	4.44822	0.453592	1

粘度　1 Pa·s(N·s/m^2) = 10 P(ポアズ)(g/(cm·s))

動粘度　1 m^2/s = 10^4 St(ストークス)(cm^2/s)

圧力	MPa(=10 bar)	kgf/cm^2	atm	mmHg(Torr)	lbf/in^2(psi)
	1	10.1972	9.86923	7.50062 × 10^3	145.038
	0.0980665	1	0.967841	735.559	14.2233
	0.101325	1.03323	1	760	14.6959
	1.33322 × 10^{-4}	1.35951 × 10^{-3}	1.31579 × 10^{-3}	1	1.93368 × 10^{-2}
	6.89476 × 10^{-3}	7.03070 × 10^{-2}	6.80460 × 10^{-2}	51.7149	1

エネルギー・仕事・熱量	J(=10^7 erg)	kgf·m	kW·h	cal(計量法)	Btu	ft·lbf	eV
	1	0.101972	2.77778 × 10^{-7}	0.238889	9.47813 × 10^{-4}	0.737562	6.24150 × 10^{18}
	9.80665	1	2.72407 × 10^{-6}	2.34270	9.29487 × 10^{-3}	7.23301	6.12082 × 10^{19}
	3.6 × 10^6	3.67098 × 10^5	1	8.59999 × 10^5	3412.13	2.65522 × 10^6	2.24694 × 10^{25}
	4.18605	0.426858	1.16279 × 10^{-6}	1	3.96759 × 10^{-3}	3.08747	2.61272 × 10^{19}
	1055.06	107.586	2.93072 × 10^{-4}	252.042	1	778.172	6.58515 × 10^{21}
	1.35582	0.138255	3.76616 × 10^{-7}	0.323890	1.28506 × 10^{-3}	1	8.46233 × 10^{18}
	1.60218 × 10^{-19}	1.63377 × 10^{-20}	4.45050 × 10^{-26}	3.82743 × 10^{-20}	1.51857 × 10^{-22}	1.18171 × 10^{-19}	1

1 cal = 4.18605 J（計量法）

= 4.184 J　（熱化学）

= 4.1855 J（15 °C）

= 4.1868 J（国際蒸気表）

仕事率　1 PS（仏馬力）

= 75 kgf·m/s

= 735.499 W

放射能	Bq	Ci
	1	2.70270 × 10^{-11}
	3.7 × 10^{10}	1

吸収線量	Gy	rad
	1	100
	0.01	1

照射線量	C/kg	R
	1	3876
	2.58 × 10^{-4}	1

線量当量	Sv	rem
	1	100
	0.01	1

（86 年 12 月 26 日現在）

Premoderator Optimization of Decoupled Hydrogen Moderator